Development of *Escherichia coli* Platform for Tyrosine-derivative Production Using Aromatic Amino Acid Hydroxylases

（芳香族アミノ酸水酸化酵素を用いたチロシン関連化合物生産のための大腸菌の構築）

Sheng Ning

Graduate School of Chemical Sciences and Engineering

Hokkaido University

Abstract

Aromatic compounds derived from tyrosine (Tyr) are important and diverse chemicals used for industrial and commercial applications. Although these compounds can be obtained by extraction from natural producers such as plants, their growth is slow and their content is low. To overcome these problems, many of them have been chemically synthesized from petroleum-based feedstocks. However, because of the environmental burden and depleting availability of feedstock, microbial cell factories are attracting much attention as sustainable and environmentally friendly processes.

To develop microbial cell factories for Tyr and Tyr-derivative production, I constructed simple and convenient Tyr-producing *Escherichia coli* (*E. coli*) platforms with phenylalanine (Phe) hydroxylase (PheH), which converted Phe to Tyr with O_2 and tetrahydromonapterin (MH4) as a cofactor, by engineering their genes with plasmid-based and chromosome-integrated methods. For effective Tyr production from Phe, a MH4 regeneration system consist of reduction of the oxidized form of the cofactor, quinonoid dihydromonapterin, with NADH by pterin-4α-carbinolamine dehydratase (PCD) and dihydropteridine reductase (DHPR), was also constructed. The Tyr titer of the plasmid-based *E. coli* platform expressing the genes encoding PheH, PCD, and DHPR was 25.5 mM (4.63 g/L) in a medium containing 30.3 mM (5.00 g/L) Phe with a test tube. The strain was successfully used to produce a industrially attractive compound, tyrosol, with a yield of 11.5 mM (1.58 g/L) by installing additional Tyr decarboxylase (TDC) and tyramine oxidase (TYO) genes on a plasmid.

Chromosomal engineering of *E. coli* has an advantage over the use of plasmids

because it increases genetic stability without antibiotic feeding to the culture media and relieves the metabolic burden associated with plasmid maintenance. Therefore, I constructed a Tyr-producing platform strain by integration of multiple *T7* promoter-controlled genes encoding PheH1, PCD, and SKIK-tagged DHPR on different chromosome loci (strainY3). The strain produced 28.6 ± 1.1 mM Tyr (5.19 g/L; 94.4% conversion from Phe). Then, I developed a tyrosol-producing platform from strain Y3 by expressing selected tyrosine decarboxylase-, tyramine oxidase (TYO)-, and medium-chain dehydrogenase/reductase (YahK)-encoding genes, all of which were controlled by *T7* promoter and integrated into the chromosome. However, the strain produced a melanin-like pigment as a byproduct, which is suggested to be formed from 4-hydroxyphenylacetaldehyde (a TYO product/YahK substrate). By using a culture medium containing a high concentration of glycerol, which was reported to enhance NADH supply required for YahK activity, the final titer of tyrosol reached 2.42 g/L in test tube-scale cultivation with a concomitant decrease in the amount of pigment.

In conclusion, I developed *E. coli* platforms for production of Tyr and Tyr-related compounds from Phe at multi-gram-per-liter levels in test-tube cultivation by plasmid-based and chromosome-engineered methods. The platforms would be useful for production of Tyr-derivatives at multi-grams-per-liter levels in test tubes.

TABLE OF CONTENTS

Chapter 1

General introduction

1.1Background and objectives

Aromatic compounds are an important class of diverse chemicals with a wide range of industrial and commercial applications, such as nutraceuticals (vitamin E, resveratrol, hydroxytyrosol), pharmaceuticals (3,4-dihydroxyphenylalanine (DOPA), adrenalin, morphine, melatonin), fragrance ingredients (2-phenylethanol, 3-phenylpropanol), and polymers (styrene, hydroxystyrene, tyrosol) **[1–6]**. These compounds are biosynthesized by various plants, algae, fungi, and bacteria from proteinogenic amino acids, phenylalanine (Phe), tyrosine (Tyr), and tryptophan (Trp) as precursors.

Although these aromatic compounds can be obtained by extraction from producers, their growth is slow. Additionally, the content of the compounds is low. To overcome these problems, many aromatic compounds have been chemically synthesized from petroleum-based feedstocks. However, because of the environmental burden and depleting availability of feedstock, other sustainable and environmentally friendly processes are required. Recent remarkable advances in metabolic engineering and synthetic biology have made it possible to develop fermentative processes using microbial cell factories, which utilized natural and non-natural biosynthetic pathways to produce chemicals from renewable resources **[7–11]**.

Aromatic compounds derived from Tyr are important chemicals and various microbial cell factories that produce Tyr derivatives have been developed by already-known and artificially designed biosynthetic pathways that utilize enzymes/genes from different sources **[1–4]**. *Escherichia coli* (*E. coli*) and yeast have been extensively used as hosts. Several bacteria were also considered. Among the hosts, *E. coli* exhibits

considerable advantages in the rapid development of microbial cell factories suitable for industrial production because of its high growth rate and well-studied genome and metabolic network as well as the availability of various synthetic biology tools for engineering and established strategies for high-cell-density fermentation in inexpensive media **[5]**.

To develop microbial cell factories for production of Tyr derivatives, enhancement of Tyr supply in *E. coli* is essential. However, the natural Tyr production is strictly controlled at a much lower level because its biosynthesis is elaborately regulated (Figure 1-1) **[12]**. Furthermore, low solubility of Tyr (0.45 g/L, 2.5 mM in water at 25 °C) makes it difficult to feed Tyr into culture broths at high concentrations **[13]**. To increase Tyr supply, various metabolic engineering approaches, such as deregulation at transcriptional level and overexpression of bottlenecks and feedback-resistant enzymes, have been employed **[14–16]**. Although the titers by flask-scale production were reported to be 2 to 3 g/L by the rationally engineered strains, further enhanced production is necessary for industrial applications.

Tyr can be converted from Phe by Phe hydroxylase (PheH) **[17, 18]**. PheH is an iron-dependent non-heme enzyme that catalyzes *para*-hydroxylation of Phe using O_2 and tetrahydrobiopterin (BH4) as the reducing substrate (Figure 1-2). Some bacteria, including *Chromobacterium*, *Pseudomonas*, and *Xanthomonas* species, have PheHs, which use tetrahydromonapterin (MH4) instead of BH4 as the cofactor **[19, 20]**. Previously, Satoh *et al.* succeeded in engineering an *E. coli* strain that could oxidize Tyr to DOPA using mouse Tyr hydroxylase (TyrH), a PheH homolog, and endogenous MH4,

together with the human BH4 regeneration system, in which the oxidized form of the cofactor, quinonoid dihydromonapterin (qMH2), was reduced with NADH by pterin-4α-carbinolamine dehydratase (PCD) and dihydropteridine reductase (DHPR) (Figure 1-2) **[21]**. Considering a high water-solubility of Phe (179 mM, 29.6 g/L in water at 25 °C), in this study, I developed a simple and convenient Tyr-producing *E. coli* platform from Phe as an initial substrate by expressing the PheH and the human BH4 regeneration system (PCD and DHPR) with plasmids (Chapter 2). To enable more flexible pathway engineering, I also constructed a plasmid-free platform by integration of the above-mentioned genes of the PheH and the human BH4 regeneration system into the chromosome (Chapter 3). This has an advantage over the use of plasmids because it increases genetic stability without antibiotic feeding into the culture media and accepts more plasmids carrying artificial pathway genes. These platform strains were successfully applied to produce tyrosol.

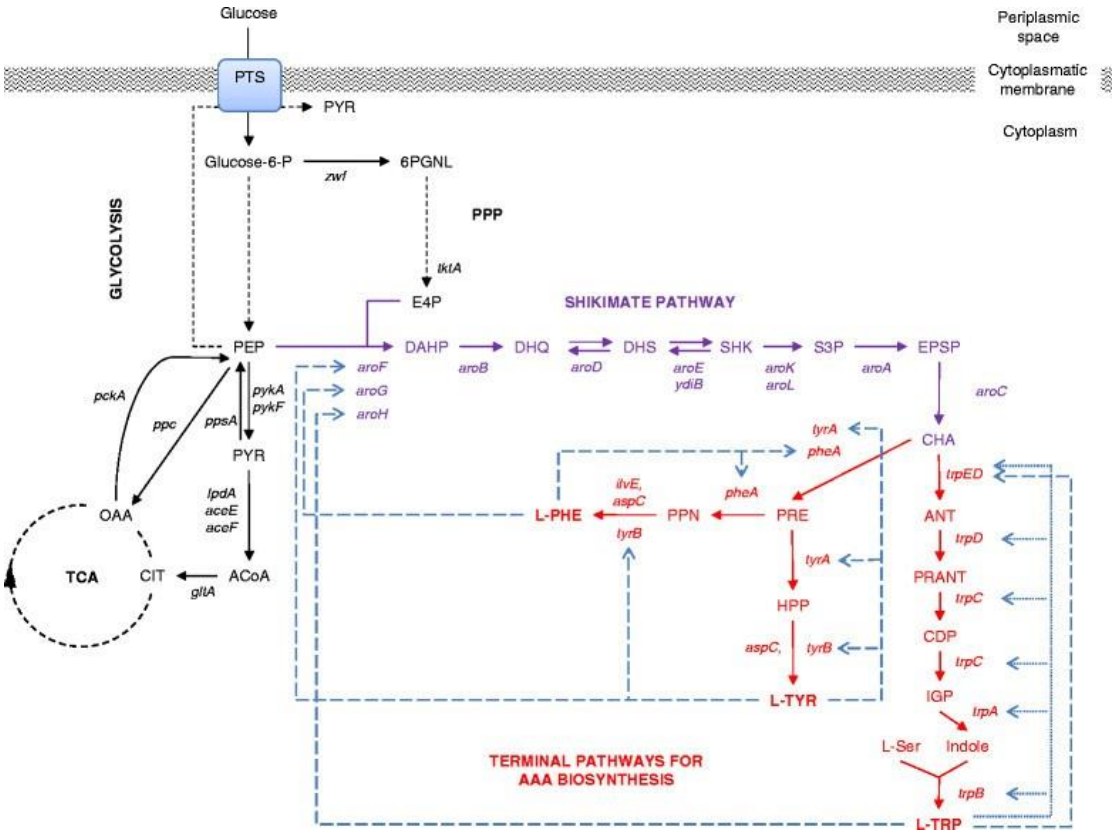

Figure 1-1. Regulation of tyrosine biosynthetic pathway. [12]

Central carbon metabolism intermediates and genes shown: PPP (pentose phosphate pathway); TCA (tricarboxylic acid cycle); E4P (erythrose-4-P); PGNL (6-phospho D-glucono-1,5-lactone); PEP (phosphoenolpyruvate); PYR (pyruvate); ACoA (acetyl-CoA); CIT (citrate); OAA (oxaloacetate); *zwf* (glucose 6-phosphate-1-dehydrogenase); *tktA* (transketolase I); *pykA*, *pykF* (pyruvate kinase II and pyruvate kinase I, respectively); *lpdA*, *aceE*, and *aceF* (coding for PYR dehydrogenase subunits); *gltA* (citrate synthase); *pckA* (PEP carboxykinase); *ppc* (PEP carboxylase); *ppsA* (PEP synthetase). Shikimate pathway intermediates and genes shown: DAHP (3-deoxy-D-*arabino*-heptulosonate-7-phosphate); DHQ (3-dehydroquinate); DHS (3-dehydroshikimate); SHK (shikimate); S3P (SHK-3-phosphate); EPSP (5-enolpyruvyl-shikimate 3-phosphate); CHA (chorismate); *aroF*, *aroG*, *aroH* (DAHP synthase AroF, AroG and AroH, respectively); *aroB* (DHQ synthase); *aroD* (DHQ dehydratase); *aroE*,

ydiB (SHK dehydrogenase and SHK dehydrogenase / quinate dehydrogenase, respectively); *aroA* (3-phosphoshikimate-1-carboxyvinyltransferase); *aroC* (CHA synthase). Terminal AAA biosynthetic pathways intermediates and genes shown: ANT (anthranilate); PRANT (*N*-(5-phosphoribosyl)-anthranilate); CDP (1-(o-carboxyphenylamino)-1'-deoxyribulose 5'-phosphate); IGP ((1S,2R)-1-C-(indol-3-yl)glycerol 3-phosphate); *trpE*, *trpD* (ANT synthase component I and II, respectively); *trpC* (indole-3-glycerol phosphate synthase / phosphoribosylanthranilate isomerase); *trpA* (indoleglycerol phosphate aldolase); *trpB* (tryptophan synthase); PRE (prephenate); PPN (phenylpyruvate); HPP (4-hydroxyphenylpyruvate); *tyrA*, *pheA* (TyrA and PheA subunits of the CHA mutase, respectively); *ilvE* (subunit of the branched-chain amino acid aminotransferase)*;* *aspC* (subunit of aspartate aminotransferase); *tyrB* (tyrosine aminotransferase). Continuous arrows show single enzymatic reactions, black dashed arrows show several enzymatic reactions, long-dashed blue arrows indicate allosteric regulation and dotted blue arrows indicate transcriptional repression.

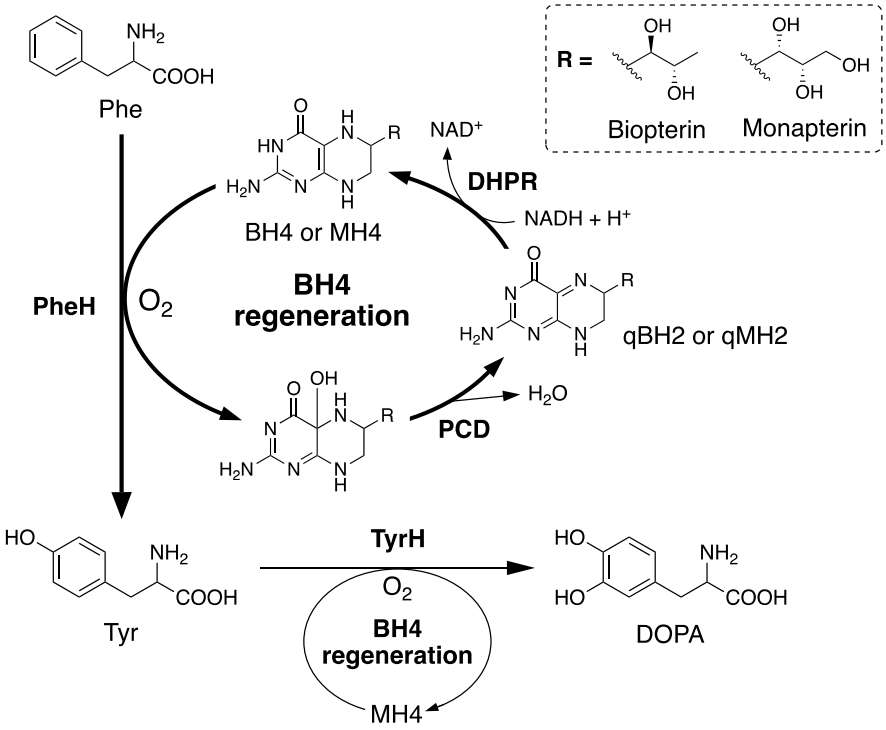

Figure 1-2. Reactions of phenylalanine and tyrosine hydroxylases.

Phe (phenylalanine); Tyr (tyrosine); DOPA (3,4-dihydroxyphenylalanine); BH4 (tetrahydrobiopterin); MH4 (tetrahydromonapterin); qMH2 (quinonoid dihydromonapterin); qBH2 (quinonoid dihydrobiopterin); DHPR (dihydropteridine reductase); PCD (pterin-4α-carbinolamine dehydratase); PheH (phenylalanine hydroxylase); TyrH (tyrosine hydroxylase).

1. 2 Target compound, tyrosol

Tyrosol is a natural polyphenol found in olive oil, sake, wine, and have been reported to promote human health due to their anti-atherogenic, cardioprotective, anti-tumor, neuroprotective, anti-diabetic, and anti-obesity activities **[22–25]**. Tyrosol can be used for the preparation of commercially available pharmaceutical agents such as betaxolol **[26]** and metoprolol **[27]**, which are selective β1 receptor blockers and used in the treatment of hypertension, angina, heart failure, and glaucoma **[28]**. Recently, tyrosol was reported to be attractive for a biobased and nontoxic phenolic building block of a thermosetting resin **[29]**. For industrial purposes, tyrosol is chemically produced.

Chapter 2

Plasmid-based Tyr-producing platform and its application

2.1 Introduction

To develop microbial cell factories for production of Tyr derivatives, I developed a simple and convenient Tyr-producing *E. coli* platform, which converted Phe to Tyr with PheH, O_2 and a cofactor MH4, using a synthetic biology approach (Figure 2.1-1) **[30]**. For construction of the platform, a human BH4 regeneration system to regenerate MH4, which is stoichiometrically consumed during the Phe hydroxylation reaction, with NADH was installed into *E. coli* using plasmid pSTV-BH4R containing a *PCD–DHPR* operon under the control of *lac* promoter. The thus constructed strain was used to search for PheHs with high activities. As a result, the plasmid-based engineered strain with *Gulbenkiania* sp. *PheH1* gene produced 25.5 mM (4.63 g/L) Tyr in a medium initially including 30.3 mM (5.00 g/L) Phe in test-tube scale. Furthermore, the *E. coli* platform was evaluated for tyrosol production by introducing their biosynthetic genes and 11.5 mM (1.58 g/L) of tyrosol was yielded **[30, 31]**. Thus, the constructed platform would be useful for evaluation of microbial cell factories installing various designed Tyr-derivative biosynthetic pathways at multi-grams-per-liter levels in test tubes.

In this chapter, the details of the experiments are described.

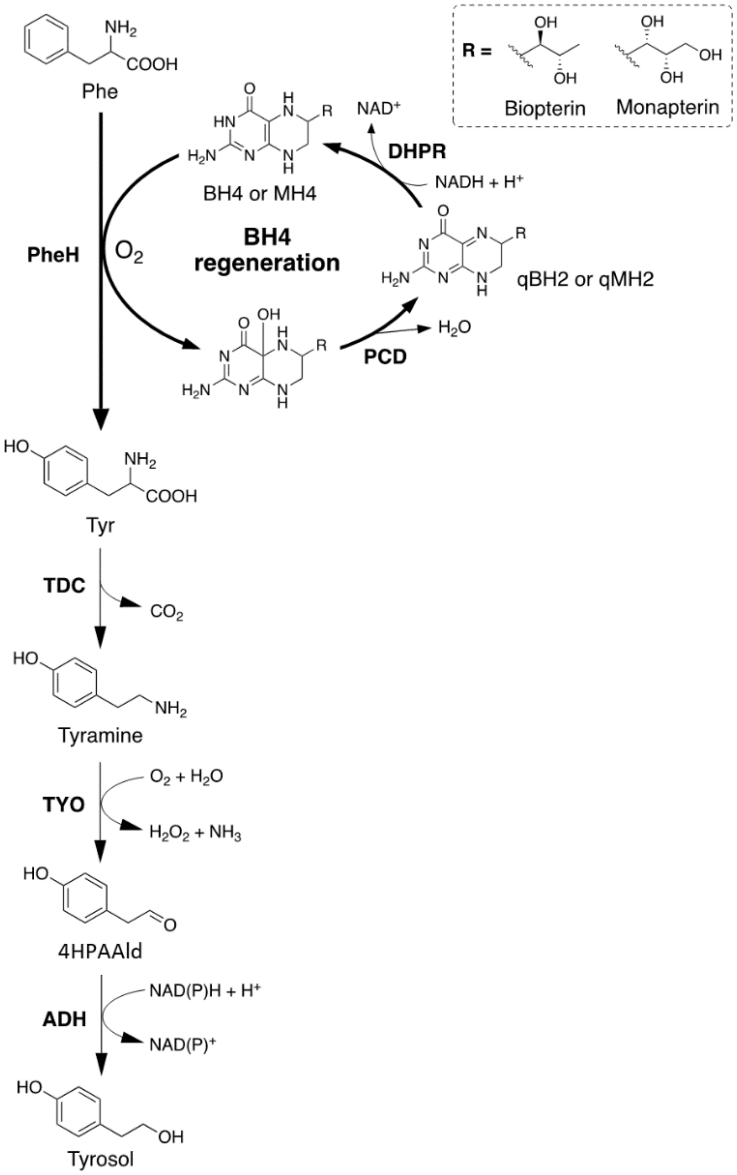

Figure 2.1-1. Biosynthetic pathway for producing tyrosine and tyrosol from phenylalanine.

Phe (phenylalanine); Tyr (tyrosine); BH4 (tetrahydrobiopterin); MH4 (tetrahydromonapterin); qMH2 (quinonoid dihydromonapterin); qBH2 (quinonoid dihydrobiopterin); 4HPAAld (4-hydroxyphenylacetaldehyde); PheH (phenylalanine hydroxylase); DHPR (dihydropteridine reductase); PCD (pterin-4α-carbinolamine dehydratase); TDC (Tyr decarboxylase); TYO (tyramine oxidase); ADH (alcohol dehydrogenase).

2.2 Results

2.2.1 Tyr-producing platform using plasmids

2.2.1.1 Screening of PheH for Tyr-overproduction

For construction of an *E. coli* platform to produce Tyr from Phe at a high titer, I searched for PheHs with high activities. To estimate the net effect of PheH activity for Tyr production, a Tyr-auxotrophic mutant *E. coli* strain Y0 was used as the host, in which the *tyrA* gene encoding the bifunctional chorismate mutase/prephenate dehydratase was knocked out **[32]**. For regeneration of the cofactor MH4, which is consumed during the Phe hydroxylation reaction in stoichiometric amounts, the human pterin-4α-carbinolamine dehydratase (PCD) and dihydropteridine reductase (DHPR) genes were co-expressed as an operon in this order under the control of a *lac* promoter using pSTV-BH4R (*lac* promoter, *PCD–DHPR* operon, p15A ori, Cm^R; Figure 2.2.1.1-1). Their expression as soluble forms in the strain Y0 harboring pSTV-BH4R (strain YBR) was confirmed by western blot analysis (Figure 2.2.1.1-2).

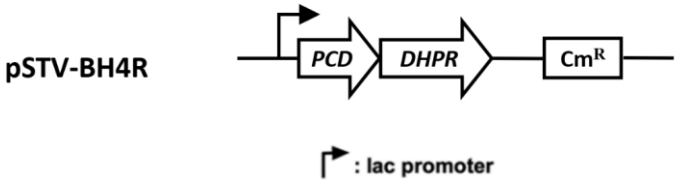

Figure 2.2.1.1-1. Gene organization in the constructed plasmid pSTV-BH4R for cofactor BH4/MH4 regeneration.

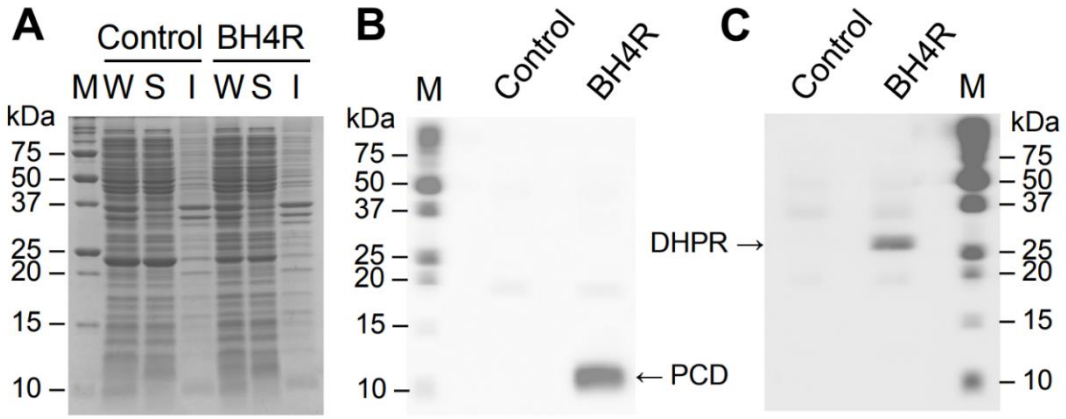

Figure 2.2.1.1-2. Sodium dodecyl sulfate–polyacrylamide gel electrophoresis (SDS-PAGE) (A) and western bolt (B and C) analyses of PCD and DHPR production.
(A) Whole cell (W), soluble (S), and insoluble (I) fractions prepared from strain Y0 harboring empty vector pSTV28N (Control) and pSTV-BH4R (BH4R) were analyzed by SDS-PAGE. Marked PCD (12.0 kDa) and DHPR (25.8 kDa) production was not confirmed on the gel. M shows a marker, and the apparent molecular weights of the bands are represented. **(B)** PCD and **(C)** DHPR in the soluble fractions used in (A) were detected with anti-PCD and anti-DHPR antibodies. Detected proteins are indicated by the arrows. M also shows a marker.

Then, the activity of rat PheH (RatPheH) was examined because the enzyme was well characterized and has been successfully expressed as an active form in *E. coli* **[17, 33]**. The RatPheH consists of a regulatory domain at the *N*-terminus and a catalytic domain at the *C*-terminus. Previously, a truncated enzyme lacking the regulatory domain was found to have comparable activity to the full-length enzyme and to be highly expressed in *E. coli*. Therefore, a codon-optimized DNA fragment encoding only the catalytic domain of RatPheH (RatPheHc) was synthesized and cloned into the protein expression vector pQE1a-Red (*lac* promoter, DsRed monomer-encoding gene, *lacI*, ColE1 ori of pBR322, Ap^R) to construct pQE1a-RatC, in which the gene was expressed under the control of the *tac* promoter and repressed by *lac* operator and *lac* repressor (LacI) (Figure 2.2.1.1-3A). The soluble expression of RatPheHc in strain YBR harboring pQE1a-RatC was confirmed by sodium dodecyl sulfate–polyacrylamide gel electrophoresis (SDS-PAGE) (Figure 2.2.1.1-3B). To evaluate Tyr production, the transformant was cultured in M9Y medium, including 30.3 mM (5.00 g/L) Phe and 1.0% (w/v) glucose, for 48 h of cultivation in test tubes, and the products were analyzed by high-performance liquid chromatography (HPLC). As a result, 0.44 ± 0.03 mM (0.08 g/L) of Tyr was produced but almost all Phe was remained (Figure 2.2.1.1-4A). Therefore, the low conversion rate must be improved.

For further improvement of the conversion rate from Phe to Tyr, I focused on NADH-supply because NADH is used for reduction of the oxidized form of cofactor qMH2 during the Phe hydroxylation reaction. It has been reported that glycerol regenerates NADH more effectively than glucose **[34, 35]**; thus, glycerol was used as

the sole carbon source instead of glucose. Although the Tyr titer was improved to 1.09 ± 0.19 mM (0.20 g/L), a significant amount of Phe remained in the culture broths (Figure 2.2.1.1-4B). In addition, after 24 h of cultivation, cell growth was slower than that with glucose. Therefore, I searched for PheH with higher activity from other sources.

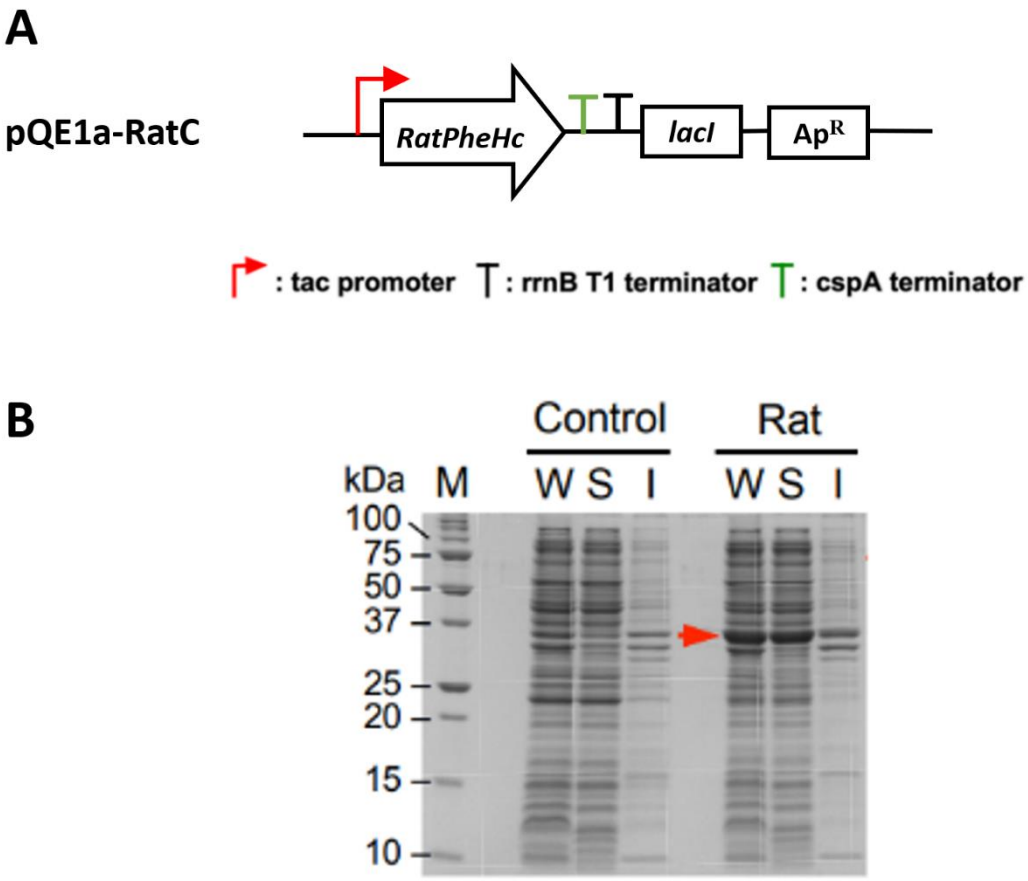

Figure 2.2.1.1-3. Gene organization in the constructed plasmid pQE1a-RatC and SDS-PAGE analysis of RatPheHc expression.

(A) Gene organization in the constructed plasmid pQE1a-RatC. **(B)**Whole cell (W), soluble (S), and insoluble (I) fractions prepared from strain YBR harboring empty vector pQE1a (Control) and pQE1a-RatC were analyzed. The soluble fraction of the catalytic domain of RatPheH (RatPheHc) was confirmed on the gel (38.6 KDa). M shows a marker.

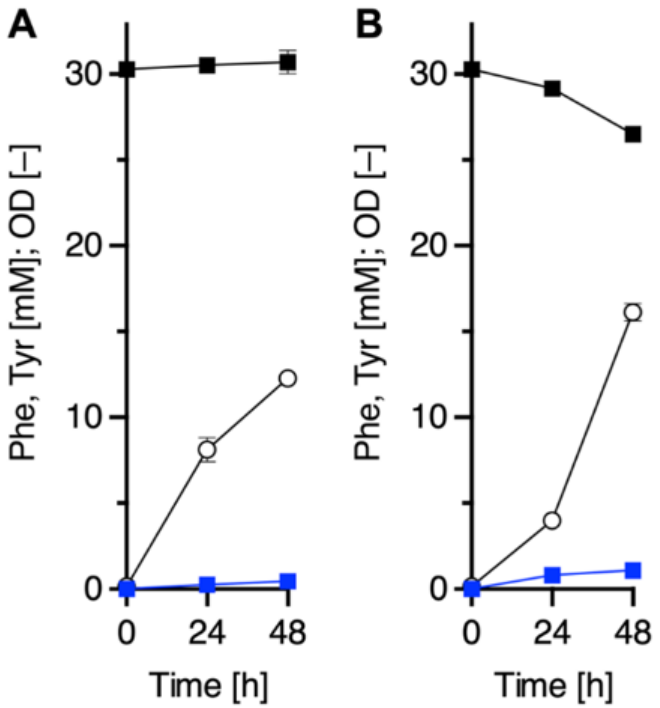

Figure 2.2.1.1-4. Tyrosine production of the engineered plasmid-based tyrosine-producing strains with rat phenylalanine hydroxylase.

Strain YBR expressing the catalytic domain of RatPheH (RatPheHc), using **(A)** glucose or **(B)** glycerol as the carbon sources. Phe, black squares; Tyr, blue squares; optical density (OD), white circles. Data are presented as mean values with standard deviations for three independent experiments.

To further improve the Tyr conversion rate, seven bacterial PheHs from different genera were screened, including *Bacillus* sp. INT005 (Bs), γ-proteobacteria *Xanthomonas oryzae* (Xo) and *Pseudomonas putida* (Pp), β-proteobacteria *Chromobacterium violaceum* (Cv), *Cupriavidus necator* (Cn), and *Gulbenkiania* sp. SG4523 (Gs1, Gs2). The identities of amino acid sequences of PheHs among these enzymes are 20% to 70% (Table 2.2.1.1-1). PCR amplified-DNA fragments encoding PheHs were cloned into the protein expression vector pQE1a-Red (Figure 2.2.1.1-5) and used for Tyr production in the same manner as described before. As shown in Figure 2.2.1.1-6, the soluble expression of all enzymes was confirmed by SDS-PAGE analysis. In terms of Tyr production, a strain YBR carrying *GsPheH1* gene yielded the highest titer (24.7 ± 1.30 mM, 4.48 g/L) among the tested PheHs at 48 h of cultivation (Figure 2.2.1.1-7). Therefore, GsPheH1 was selected for further analysis.

Table 2.2.1.1-1. Identities (%) of amino acid sequences of PheHs.

	BsPheH	RatPheH	GsPheH1	PpPheH	XoPheH	GsPheH2	CvPheH	CnPheH
BsPheH	100.0	25.4	32.9	30.1	29.8	29.6	30.0	29.1
RatPheH	25.4	100.0	31.0	27.1	29.2	29.8	27.8	24.2
GsPheH1	32.9	31.0	100.0	41.6	41.9	43.4	42.9	42.3
PpPheH	30.1	27.1	41.6	100.0	41.7	43.5	43.5	43.4
XoPheH	29.8	29.2	41.9	41.7	100.0	50.0	59.2	57.1
GsPheH2	29.6	29.8	43.4	43.5	50.0	100.0	62.7	54.3
CvPheH	30.0	27.8	42.9	43.5	59.2	62.7	100.0	67.7
CnPheH	29.1	24.2	42.3	43.4	57.1	54.3	67.7	100.0

The amino acid sequences of PheHs were analyzed using Clustal Omega program (https://www.ebi.ac.uk/Tools/msa/clustalo/).

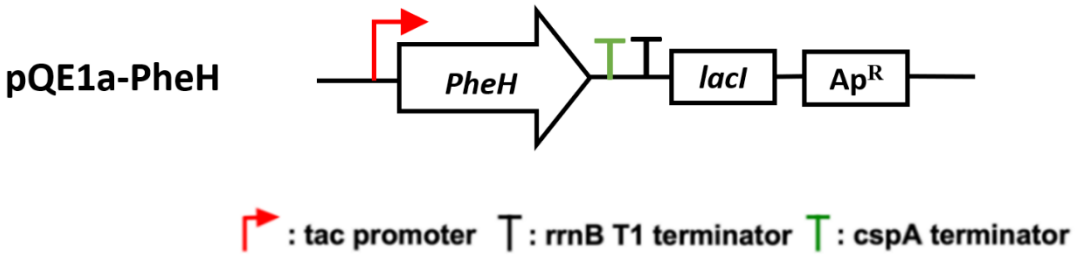

Figure 2.2.1.1-5. Gene organization in the constructed plasmids for PheH screening and tyrosine production.

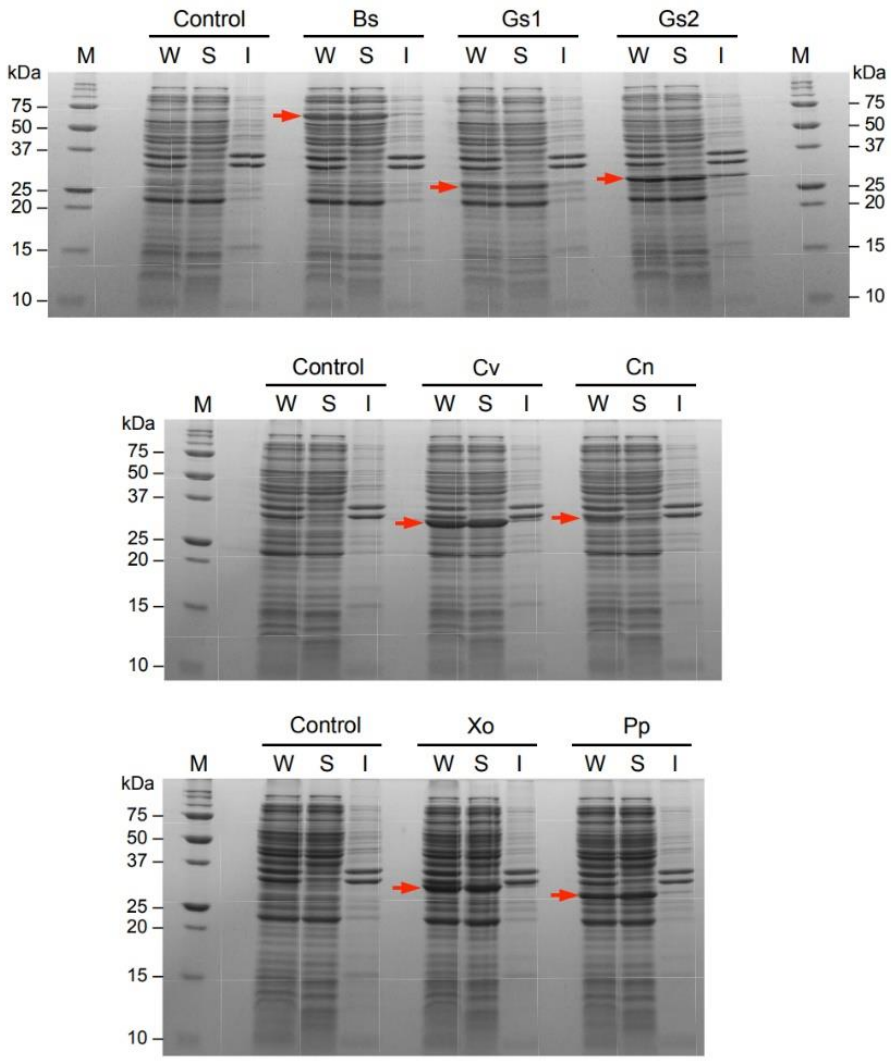

Figure 2.2.1.1-6. SDS-PAGE analysis of bacterial PheHs expression.

Whole cell (W), soluble (S), and insoluble (I) fractions of strain YBR harboring empty vector pQE1a (Control), pQE1a-Bs (Bs), pQE1a-Gs1 (Gs1), pQE1a-Gs2 (Gs2), pQE1a-Cv (Cv), pQE1a-Cn (Cn), pQE1a-Xo (Xo), or pQE1a-Pp (Pp) were analyzed by SDS-PAGE, respectively. M represents the marker, and the apparent molecular weights of the bands are indicated to the left of each gel. PheHs expressions were indicated by the red arrows. BsPheH, 64.4 kDa; GsPheH1, 29.7 kD; GsPheH2, 32.3 kDa; CvPheH, 33.6 kDa; CnPheH, 34.9 kDa; XoPheH, 33.4 kDa; PpPheH, 30.1 kDa.

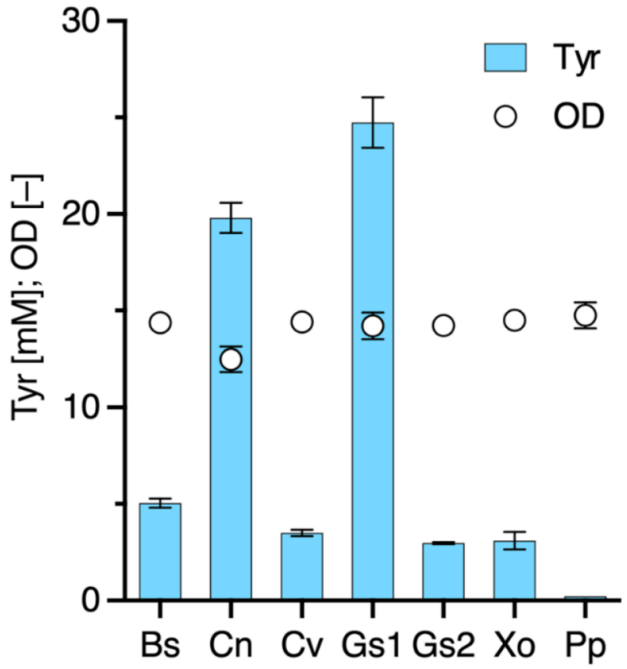

Figure 2.2.1.1-7. Tyrosine production of plasmid-based engineered strains with bacterial phenylalanine hydroxylases.

The tyrosine productivities of strain YBR harboring pQE1a derivatives including the examined bacterial *PheHs* were shown. Glycerol was used as the carbon source. BsPheH, Bs; CnPheH, Cn; CvPheH, Cv; GsPheH1, Gs1; GsPheH2, Gs2; XoPheH, Xo; PpPheH, Pp; OD, circles; Tyr, bars.

2.2.1.2 Construction of plasmid-based Tyr-producing platform

To construct pathways for Tyr-derivative production, many pathway genes were introduced into the host cell. From this point of view, the number of plasmids carrying genes encoding PheH and cofactor regeneration enzymes should be minimal. Therefore, I constructed plasmid pQE1a-Gs1-BH4R (Figure 2.2.1.2-1), which co-expressed *GsPheH1* and the BH4-regeneration genes (*PCD* and *DHPR*). As shown in Figure 2.2.1.2-2, strain Y0 harboring pQE1a-Gs1-BH4R (strain PGs) converted most of the Phe to Tyr, 25.5 ± 1.6 mM (4.63 g/L) after 48 h of cultivation. The cell growth and Tyr titer (24.2 ± 1.7 mM, 4.39 g/L) at 24 h of cultivation were markedly improved when compared with those of strain YBR harboring pQE1a-Gs1. Therefore, a plasmid-based Tyr-producing platform was successfully constructed.

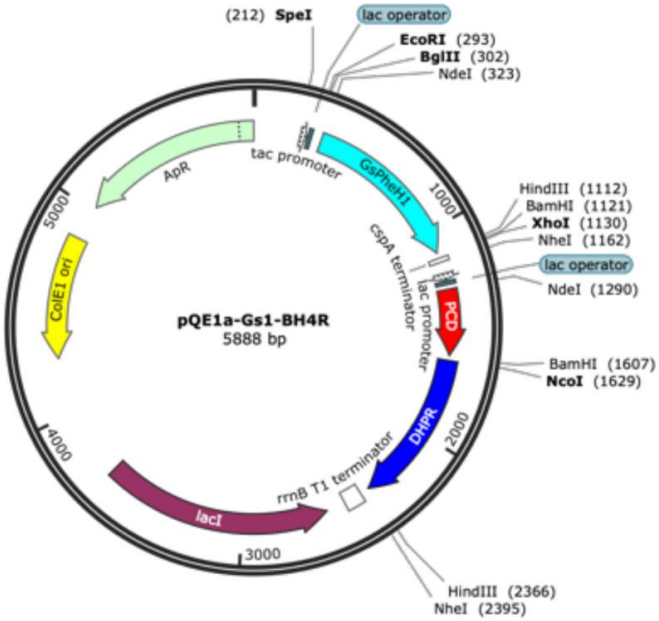

Figure 2.2.1.2-1. The plasmid map of pQE1a-Gs1-BH4R.

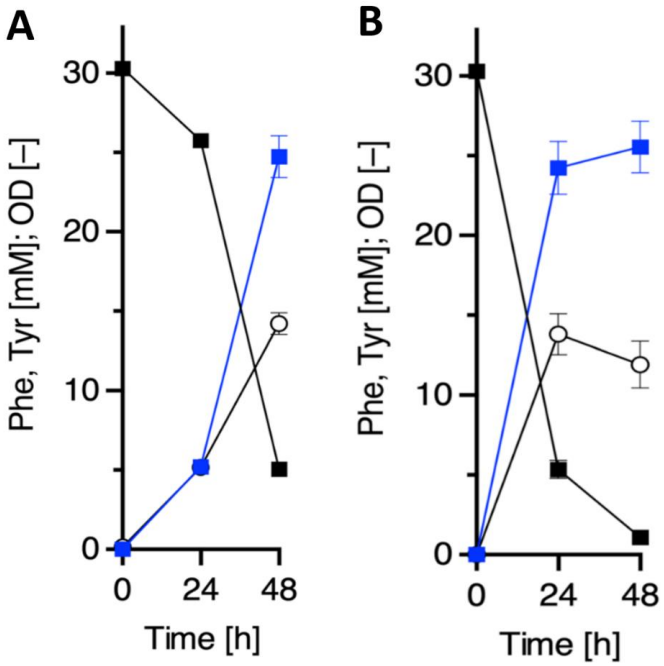

Figure 2.2.1.2-2. Tyrosine production of strain YBR harboring pQE1a-Gs1 (A) and strain PGs (B).

Phe, black squares; Tyr, blue squares; OD, white circles. Data are presented as mean values with standard deviations for three independent experiments.

2.2.2 Application of a plasmid-based Tyr-producing platform for tyrosol production

The constructed plasmid-based Tyr-producing platform (strain PGs) was applied for tyrosol production. The biosynthetic pathway for tyrosol production used in this study has three catalytic steps, decarboxylation of Tyr to tyramine, deamination of tyramine to 4-hydroxyphenylacetaldehyde (4HPAAld), and reduction of 4HPAAld to tyrosol (Figure 2.1-1) **[30, 31]**. For tyrosol production, two genes encoding Tyr decarboxylase of *Papaver somniferum* (PsTDC) and tyramine oxidase (MlTYO) of *Micrococcus luteus* were introduced into the strain PGs. The final reduction of 4HPAAld could be catalyzed by the endogenous alcohol dehydrogenases (ADHs) in *E. coli*. The PsTDC- and MlTYO-encoding genes were cloned as artificial operons into pCF1s-Red (*tac* promoter, DsRed-monomer gene, *lacI,* CloDF13 ori, Sm^R), so that the order of the two genes was interchanged to make pCF1s-TDC-TYO and pCF1s-TYO-TDC, respectively (Figure 2.2.2-1). To evaluate tyrosol production, the transformants were cultured in M9Y medium with 30.3 mM (5.00 g/L) Phe for 72 h-cultivation at 30 ºC and the broths were analyzed by HPLC. As shown in Figure 2.2.2-2, strain PGs harboring pCF1s-TYO-TDC produced 4.93 ± 0.31 mM (0.682 g/L) tyrosol, while strain PG harboring pCF1s-TDC-TYO yielded 11.5 ± 1.2 mM (1.58 g/L), which is 2.3-fold that of the former strain. The results suggested that the gene order in the operon was crucial for increasing tyrosol titer. Thus, I demonstrated that the constructed platform could be applicable for production of Tyr-derivatives.

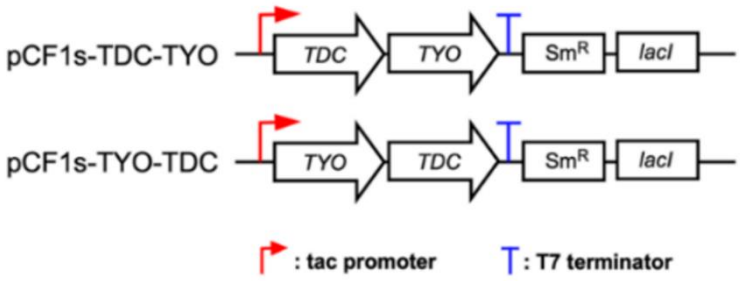

Figure 2.2.2-1. Gene organization in the constructed plasmids for tyrosol production.

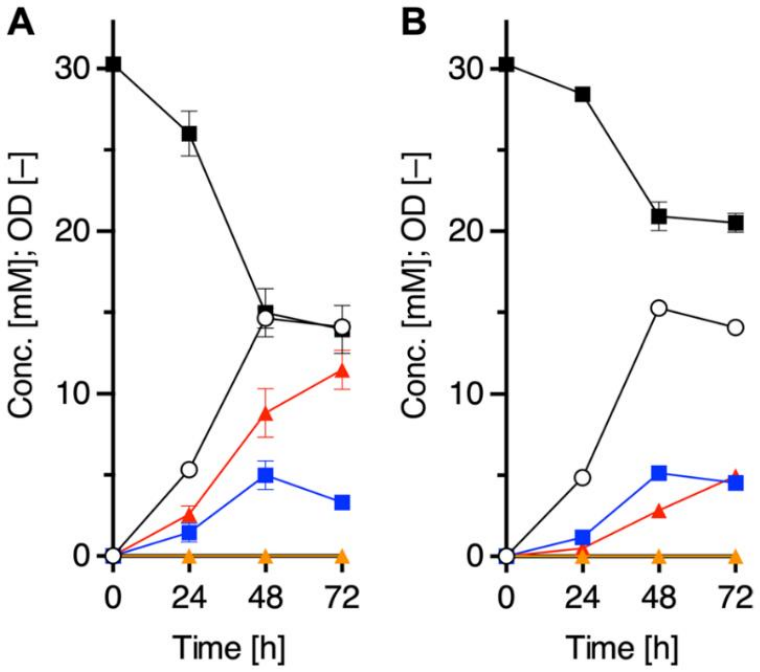

Figure 2.2.2-2. Tyrosol production of plasmid-based engineered strains. Fermentation profiles of tyrosol production of strain PGs harboring pCF1s-TDC-TYO **(A)** and pCF1s-TYO-TDC **(B)**. Each of the transformants was cultured up to 72 h at 30°C. Phe, black squares; Tyr, blue squares; tyramine, orange triangles; tyrosol, red triangles; OD, white circles. Data are presented as mean values with standard deviations for three independent experiments.

2.3 Discussion

The aim of this research was to develop simple and convenient Tyr-producing *E. coli* platforms. In chapter 2, I succeeded in development of an *E. coli* platform for production of Tyr from Phe, using *Gulbenkiania* sp. PheH1 together with human BH4-regeneration system, at multigram-per-liter levels in test tubes. The Tyr production (25.5 mM, 4.63 g/L) using the constructed plasmid-based strain PGs was higher than those of an engineered Tyr-overproducing strains in flask cultivation (16.6 mM, 3.0 g/L) **[16]**. In addition, the developed platform strain was successfully applied for production of tyrosol **[30]**. By optimization of the tyrosol-producing module, the titer was enough higher than those of previous reports **[16, 25]**. Therefore, the engineered strain would be useful for the platform of production for known and artificially designed Tyr-related compounds.

2.4 Materials and methods

2.4.1 General

All media, chemicals, and reagents were of analytical grade and were purchased from FUJIFILM Wako Pure Chemical Corporation (Osaka, Japan), Sigma-Aldrich Japan K.K. (Tokyo, Japan), KANTO CHEMICAL Co., Inc. (Tokyo, Japan), or Tokyo Chemical Industry Co., Ltd. (Tokyo, Japan).

Synthetic genes were purchased from Integrated DNA Technologies, Inc. (Coralville, IA, USA). PCR was performed using a GeneAmp PCR System 9700 thermal cycler (Thermo Fisher Scientific Inc., Waltham, MA, USA) with KOD DNA polymerase (Toyobo Co. Ltd, Osaka, Japan) according to the protocols of manufacturers. General genetic manipulations of *E. coli* were performed according to standard protocols.

2.4.2 Bacterial strains and culture conditions

Escherichia coli JM109 (Nippon Gene Co., Ltd, Tokyo, Japan) was routinely used for plasmid construction. For production of Tyr and its derivatives, *E. coli* BW25113 (National Institute of Genetics, Shizuoka, Japan) derivatives were used.

Genes of *CnPheH* and *XoPheH* were obtained from *Cupriavidus necator* H16 ATCC 17699 (American Type Culture Collection, Manassas, VA, USA) and *Xanthomonas oryzae* MAFF 311018 (National Agriculture and Food Research Organization, Ibaraki, Japan), respectively. *Bacillus* sp. INT005 FERM P-18327 (for *BsPheH*), *Pseudomonas putida* KT2440 NBRC 100650 (for *PpPheH*), and

Gulbenkiania sp. SG4523 NBRC 113456 (for *GsPheH1* and *GsPheH2)* were obtained from National Institute of Technology and Evaluation (NITE, Tokyo, Japan).

The growth medium used was LB broth medium (Lennox; Sigma-Aldrich Japan K.K.). The M9Y medium used for Tyr production was consisted of M9 minimal salts (Becton, Dickinson and Company, Franklin Lakes, NJ, USA), 0.4 or 1.0%(w/v) carbon sources (glucose or glycerol), 5 mM $MgSO_4$, 0.1 mM $CaCl_2$, and also supplemented with 0.1% (w/v) yeast extract. To maintain the plasmids, antibiotics, ampicillin (Ap), chloramphenicol (Cm), streptomycin (Sm), and kanamycin (Km) were added to media at 100, 30, 20, and 25 mg/L, respectively. For the selection of gene knockout mutants, Km was used at 13 mg/L.

2.4.3 Screening of PheHs

Polymerase chain reaction (PCR) amplified-DNA fragments encoding PheHs were cloned into the protein expression vector pQE1a-Red and used for Tyr production, respectively. The constructed plasmids, pQE1a-RatC, pQE1a-Bs, pQE1a-Cn, pQE1a-Cv, pQE1a-Gs1 and pQE1a-Gs2, pQE1a-Pp, pQE1a-Xo, were introduced in the host *E. coli* Δ*tyrA* (Tyr auxotrophy) harboring pSTV-BH4R. The transformants were cultured in M9Y medium for 48-h incubation in test tube-scale. Samples were taken for HPLC analysis at 24 and 48 h.

2.4.4 Production of tyrosol

The *E. coli* strains harboring appropriate plasmids were pre-cultured in M9Y medium containing 0.4%(w/v) glucose or glycerol for 16 h at 30°C. After inoculating appropriate amounts of the precultures into 3 mL of M9Y medium so that optical density (OD) at 600 nm to 0.15, they were incubated at 30°C with 200rpm rotation speed of shaking. The medium contained 5.00 g/L (30.3 mM) Phe, 20 mg/L $FeSO_4 \cdot 7H_2O$, and 10 g/L (1.0%[w/v]) of the same carbon sources used for pre-cultivation with test tubes. To induce protein expression, isopropyl β-D-1-thiogalactopyranoside (IPTG) was added to a final concentration of 500 μM at 4 h of cultivation, unless noted otherwise. Samples (300 μL) were collected at appropriate time-points and were analyzed by HPLC. OD measurements at 600 nm were also taken using a NanoDrop 2000C spectrophotometer (Thermo Fisher Scientific Inc.), using cuvettes after dilution in a 1 N HCl solution.

2.4.5 HPLC analysis

Culture aliquots (50 μL) mixed with 1 N HCl (200 μL) were heated at 50°C for 30 min. After centrifugation, the supernatants (2 μL) were analyzed using a Shimadzu HPLC system (Shimadzu Co., Kyoto, Japan), equipped with an Inert Sustain C18 column (column length, 150 mm; inner diameter, 2.1 mm; particle size, 3 μm; GL Science Inc., Tokyo, Japan). Buffer A (0.1%[v/v] formic acid solution) and buffer B (methanol with 0.1%[v/v] formic acid) were used as a mobile phase, and compounds were eluted at 35°C and a flow rate of 0.2 mL/min, with increasing concentrations of

buffer B as follows: 2%, 0−3 min; 2–30%, 3–35 min. Eluted compounds were detected by measuring absorbance at 210 and 280 nm.

Chapter 3

Application of plasmid-free Tyr-producing platform

3.1 Introduction

Chromosomal engineering of *E. coli* has an advantage over the use of plasmids because it increases genetic stability without antibiotic feeding to the culture media and relieves the metabolic burden associated with plasmid maintenance **[16, 36]**. In addition, it enables flexible pathway engineering because more plasmids carrying artificial pathway genes are acceptable. Therefore, in my laboratory, plasmid-free Tyr-producing platform *E. coli* strains were constructed with *lac/tac* promoter-controlled *GsPheH1* and BH4-regeneration-related genes, both of which were integrated into the five different loci of chromosome to make strain GsBR5 **[30]**. However, the strain produced small amounts of Tyr (3.23 ± 0.09 mM (0.586 g/L)) after 48 h.

3.2 Results

3.2.1 Construction of Tyr-producing patform by chromosomal engineering with *T7* promoter expression system

Tyr productivity of strain GsBR5 was only 3.23 mM (0.586 g/L) **[30]**. The low titer is likely because of the low copy number of the module genes. Therefore, high gene expression is essential for industrial use. To enhance expression of the genes integrated into the chromosome, I employed the *T7* promoter, which is stronger than the *tac* and *lac* promoters **[37]**. Chromosomal engineering was performed using a combination of Red-mediated recombination, FLP/FRT recombination, and P1 phage transduction, as described in chapter 3.4 **[38]**. To replace both promoters in the original Tyr-producing module, in which the *Gulbenkiania* sp. *PheH1* gene and the PCD–DHPR-encoding operon were controlled by the *tac* and *lac* promoters, respectively (Figure 2.2.1.2-1) **[30]**, with the *T7* promoter, PCR-amplified *PheH1* and the PCD–DHPR-encoding operon were respectively cloned downstream of two independent *T7* promoters in vector pETDuet-FRT **[38]**. The modified Tyr-producing module was integrated into the locus of *ascF*, which encoded a β-glucoside-specific phosphotransferase system enzyme II, of the chromosome of *E. coli* MG1655(DE3) to create strain Y1, because the locus has been used for successful overexpression of genes and no harmful influence was observed by their deletion **[16, 38]**. *E. coli* MG1655(DE3) produced no detectable Tyr when cultured in medium supplemented with 30.3

mM (5.00 g/L) Phe for 48 h (Figure 3.2.1-1A); strain Y1 produced 2.47 ± 0.10 mM (0.447 g/L) Tyr (Figure 3.2.1-1B) **[39]**. This was approximately 10 times the amount produced by the strain carrying the *tac* and *lac* promoter-controlled Tyr-producing module on the chromosome (GsBR1; 0.252 mM, 0.046 g/L) **[30]**, demonstrating that application of the *T7* promoter was more effective in Tyr production. However, the Tyr titer was still low.

To eliminate a bottleneck step, additional PheH1-, PCD-, or DHPR-encoding genes controlled by the *T7* promoter were integrated into the locus *feaB*, which encoded phenylacetaldehyde dehydrogenase, of strain Y1. The *feaB*-deficiency, to prevent 4-hydroxyphenylacetate formation from 4HPAAld, is essential for effective tyrosol production **[16, 31]**. As shown in Figure 3.2.1-1C-E, integration of the DHPR-encoding gene drastically elevated Tyr production to 12.0 ± 2.3 mM (2.17 g/L), indicating that the reduction step from qMH2 to MH4 is rate-limiting. Previously, Ojima-Kato *et al*. reported that insertion of a DNA sequence encoding Ser–Lys–Ile–Lys (a SKIK-tag) at the 5′-end of target genes significantly improved the expression of recombinant proteins in *E. coli* and *Saccharomyces. cerevisiae* **[40]**. Therefore, I applied the SKIK-tag for high expression of DHPR. The strain in which a SKIK-tagged DHPR-encoding gene was integrated at the *feaB* locus (called strain Y2) produced 18.2 ± 0.3 mM Tyr (3.30 g/L, Figure 3.2.1-1F). Then, a second copy of the PheH1-, PCD-, or SKIK-tagged DHPR-encoding gene was integrated into the *pflBA* locus of strain Y2 (Figure 3.2.1-1G-I). In this case, the Tyr titer was enhanced to 28.6 ± 1.1 mM (5.19 g/L; 94.4% conversion from Phe), and this strain was named as strain Y3. Thus, I

successfully constructed the plasmid-free platform strain Y3 with higher Tyr productivity **[39]**.

To confirm whether the high Tyr production was originated from the use of *T7* promoter, expression level of Tyr biosynthetic enzymes in cell free extracts of strain GsBR1 **[30]** and strain Y3, in which Tyr biosynthetic genes were controlled by *lac*/*tac* promoter and *T7* promoter, respectively, were investigated by SDS–PAGE and western blot analysis. By SDS–PAGE analysis (Figure 3.2.1-2A), DHPR was highly expressed in strain Y3 probably by using *T7* promoter and SKIK-tag. The expression level of PCD was also examined by western blot analysis because one copy of its encoding gene was integrated into the chromosome of strain GsBR1 and strain Y3, but the former and latter were controlled by *lac* promoter and *T7* promoter, respectively. As shown in Figure 3.2.1-2B, higher expression of PCD was confirmed in Y3 strain.

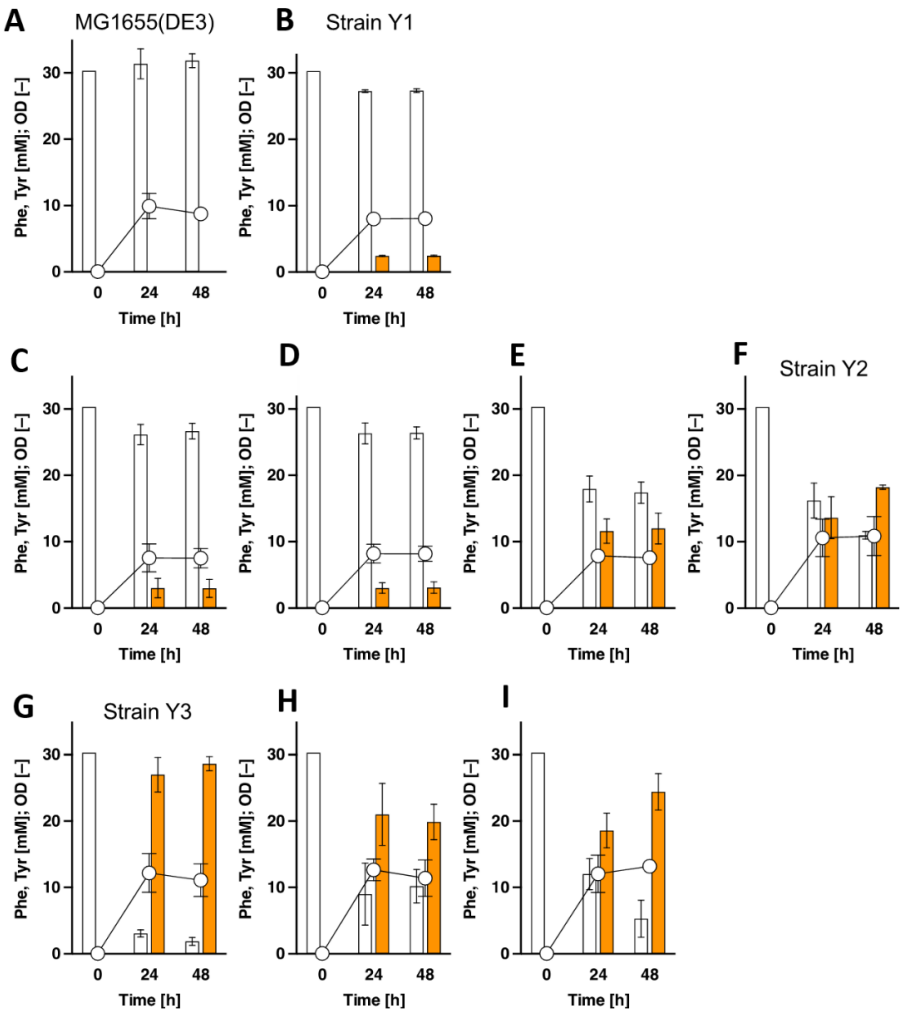

Figure 3.2.1-1. Tyrosine production in chromosome engineered strains. Tyrosine production by *E. coli* MG1655(DE3) and its derivatives, which carried Phe hydroxylase from *Gulbenkiania* sp. (PheH1)-, pterin-4α-carbinolamine dehydratase (PCD)-, and dihydropteridine reductase (DHPR)-encoding genes at different loci on the chromosome, was tested. Phe, white bars; Tyr, orange bars; OD, white circles. Each of the strains was cultured for 48 h at 30°C. **(A)** *E. coli* MG1655(DE3), **(B)** strain Y1 [*E. coli* MG1655(DE3) carrying a modified Tyr-producing module at the *ascF* locus], **(C–F)** strain Y1 carrying PheH1-, PCD-, DHPR-, and SKIK-tagged DHPR-encoding genes at the *feaB* locus, respectively; **(G–I)** strain Y2 [strain Y1 carrying SKIK-tagged DHPR-encoding gene at the *feaB* locus] carrying PheH1-, PCD-, and SKIK-tagged DHPR-encoding genes at the *pflBA* locus, respectively. Data are presented as mean values with standard deviations from three independent experiments.

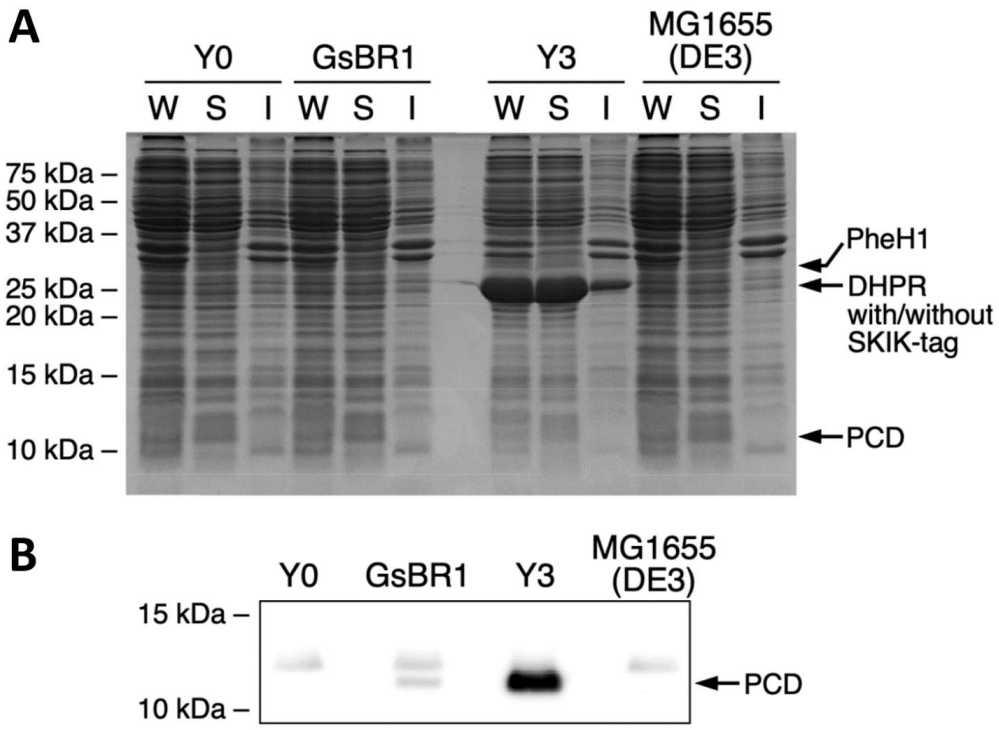

Figure 3.2.1-2. SDS–PAGE (A) and western bolt (B) analysis of protein production of tyrosine-producing strains.

(A) Whole cell (W), soluble (S), and insoluble (I) fractions prepared from strain Y0 (*E. coli* BW25113 Δ*tyrA* Δ*feaB–tynA*; control for strain GsBR1), strain GsBR1 [one copy of the original Tyr-producing module integrated into *tyrA*-knockout region in the chromosome of strain Y0], strain Y3, and strain *E. coli* MG1655(DE3) (control for strain Y3), respectively, were analyzed by SDS–PAGE. High production of DHPR in strain Y3 was confirmed. PCD, 12.0 kDa; DHPR with or without SKIK-tag, 26.2 or 25.8 kDa; PheH1, 29.7 kDa. **(B)** PCD production was compared between strains GsBR1 and Y3, both of which have one copy of integrated PCD gene, but the former and the latter were controlled by *lac* promoter and *T7* promoter, respectively. PCD in the soluble fractions used in (A) were detected with a rabbit anti-human PCD antibody as a primary antibody and a horseradish peroxidase-conjugated goat anti-rabbit IgG as a secondary antibody.

3.2.2 Application of the plasmid-free Tyr-producing platform for tyrosol production

3.2.2.1 Screening of TDC

The high Tyr-producing strain Y3 was applied for tyrosol production via the TDC-TYO pathway (Figure 2.1-1). First, I evaluated tyramine production by integrating TDC gene from *Papaver somniferum* (*PsTDC*), which was previously employed for plasmid-based tyrosol production (Chapter 2), under the control of *T7* promoter into the chromosome of strain Y3. The locus of *tyrB*, tyrosine aminotransferase gene, was used because it was previously used for expression of pathway genes **[41]**. As a result, the tyramine titer was 16.1 ± 1.1 mM (2.21 g/L) for 48 h cultivation in HCFY medium initially including 30.3 mM (5.00 g/L) Phe (Figure 3.2.2.1-1). Although almost all the Phe was consumed, 10.6 ± 0.5 mM (1.92 g/L) Tyr remained after 48 h, indicating that the TDC-catalyzed reaction was rate-limiting.

To improve the conversion rate, I searched for another TDC with higher activity in tyramine production and selected *Lactobacillus brevius* TDC (LbTDC) because it has been characterized and successfully expressed in an active form in *E. coli* **[42]**. Additionally, its S586A mutant (LbTDCm), which was reported to have 2.2-fold higher activity than the wild-type enzyme, was tested **[43]**. Table 3.2.2.1-1 shows the *in vitro* TDC activity of crude extracts prepared from *E. coli* MG1655(DE3) carrying each of the TDC-encoding genes in the chromosome.

As a result, LbTDC and LbTDCm showed higher activities than PsTDC.

The genes encoding these enzymes were then respectively transferred to strain Y3 by P1 transduction, and the transformants were cultured in the same conditions as described above. As shown in Figure 3.2.2.1-2, the strain carrying *LbTDCm* gene yielded 29.5 ± 0.3 mM (4.05 g/L; 97.4 % conversion from Phe) tyramine after 24 h of cultivation. Hence, this strain, named YD, was chosen for further analysis. In the experiments, all the tyramine-forming strains also produced tyrosol, probably because of conversion of tyramine by endogenous TYO and ADH(s) and/or aldehyde reductase(s) (AR(s)) in *E. coli* **[30, 31, 44]**.

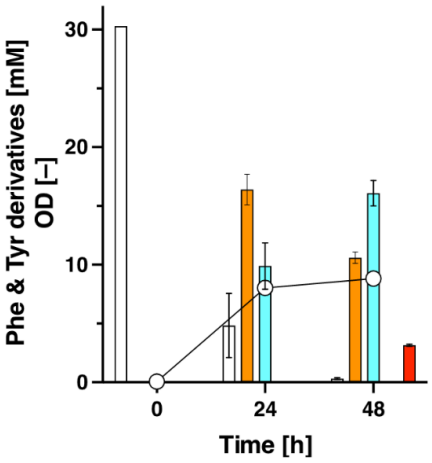

Figure 3.2.2.1-1. Tyramine production of strain Y3 integrated *Papaver somniferum* tyrosine decarboxylase (PsTDC)-encoding gene into the chromosome. Phe, white bars; Tyr, orange bars; tyramine, light-blue bars; tyrosol, red bars; OD, white circles. Data are presented as mean values with standard deviations from three independent experiments.

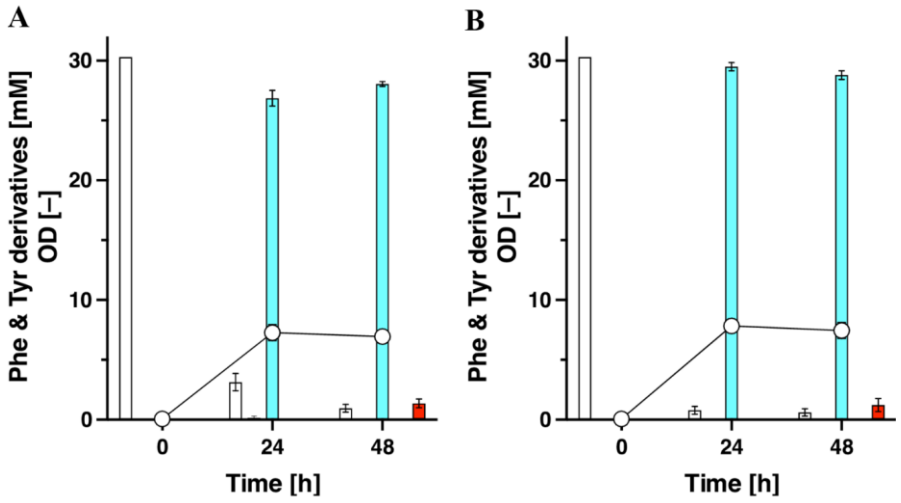

Figure 3.2.2.1-2. Tyramine production of strain Y3 integrated *Lactobacillus brevis* tyrosine decarboxylase (LbTDC)-encoding genes into the chromosome.

(A) *L. brevis* TDCs of wild type (LbTDC) and **(B)** S586A mutant (LbTDCm). Phe, white bars; Tyr, orange bars; tyramine, light-blue bars; tyrosol, red bars; OD, white circles. Data were presented as mean values with standard deviations from three independent experiments.

Table 3.2.2.1-1. Tyrosine decarboxylase activity *in vitro*.

Gene integrated	Specific activity (U/mg protein)	
	pH 5.0	pH 7.0
None	ND	ND
PsTDC	ND	0.006 ± 0.000
LbTDC	0.043 ± 0.027	0.037 ± 0.002
LbTDCm	0.093 ± 0.017	0.054 ± 0.004

ND, not detected.

The optimal pH for LbTDC enzymes is pH 5.0 **[42, 43]**.

3.2.2.2 Screening of TYO

Next, I searched for TYOs with high activities for tyrosol production. The activities of five bacterial TYOs from *Micrococcus luteus* (MlTYO), *Escherichia coli* K-12 (EcTYO), *Klebsiella aerogenes* (KaTYO), *Acinetobacter baumannii* (AbTYO), and *Brevibacterium casei* (BcTYO) were examined. Each of the genes under the control of *T7* promoter was integrated into the locus of *lacZ*, which encoded β-galactosidase gene and was previously used for expression of pathway genes **[45]**, in the chromosome of *E. coli* MG1655(DE3) and then the *in vitro* TYO activity of crude extracts prepared from the transformants was examined. As shown in Figure 3.2.2.2-1, the transformant carrying *MlTYO* gene showed the expected activity (0.022 ± 0.001 U/mg · protein) under the reaction condition. Thus, the MlTYO was selected for further analysis.

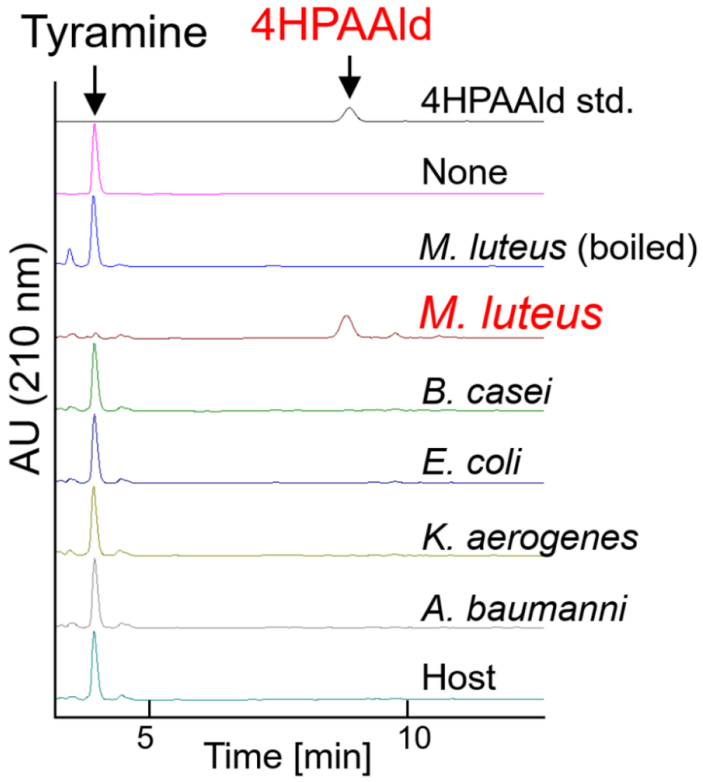

Figure 3.2.2.2-1. HPLC analysis (210 nm) of reaction mixtures of *in vitro* experiments with crude extracts including tyramine oxidases (TYO) and tyramine as a substrate.

Crude extracts were prepared from *E. coli* MG1655(DE3) carrying TYO genes from *A. baumanni*, *K. aerogenes*, *E. coli*, *B casei*, and *M. luteus*, respectively. Host, *E. coli* MG1655(DE3) without integrated TYO gene; None, no crude extract in the reaction mixture.

3.2.2.3 Tyrosol production using TDC and TYO

To convert the tyramine-producing strain YD to a tyrosol-producing strain (strain YDO), the *MlTYO* gene was integrated into the *lacZ* locus in the chromosome of strain YD by P1 transduction. The tyrosol production of strain YDO was 3.84 ± 0.73 mM (0.531 g/L) after 48 h of cultivation (Figure 3.2.2.3-1A). Considering that the tyramine titer of strain YD (29.5 ± 0.3 mM) was higher than that of tyrosol produced by strain YDO, and the tyrosol titer of strain YDO was nearly constant between 24 and 48 h, thus tyramine and/or 4HPAAld were/was suggested to be converted to undesirable shunt products by strain YDO. Indeed, the total mass of Phe, tyrosol, Tyr, tyramine, and 4HPAAld (11.2 mM) at 48 h was less than the initial amount of Phe (30.3 mM). Finally, I noticed that the color of the culture broth of strain YDO changed to brown or dark-brown depending on the cultivation time, but this phenomenon was not observed for strain YD (Figure 3.2.2.3-1B). Taking these results together, I hypothesized that 4HPAAld formed from tyramine by MlTYO was converted to a dark-brown compound.

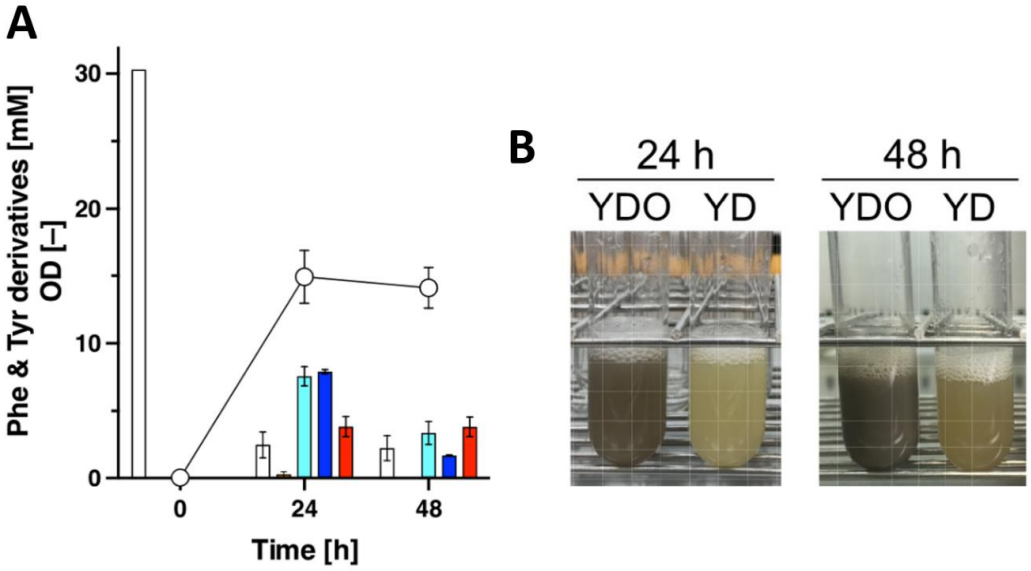

Figure 3.2.2.3-1. Tyrosol production of strain YDO.

(A) Strain YDO was cultured for 48 h at 30°C. Phe, white bars; tyramine, light-blue bars; 4HPAAld, blue bars; tyrosol, red bars; OD, white circles. Data are presented as mean values with standard deviations from three independent experiments. **(B)** Photographs of the culture broths of strains YDO and YD after 24 and 48 h of cultivation.

3.2.2.4 *In vitro* experiments with purified MlTYO

To test this hypothesis, I performed an *in vitro* experiment using purified recombinant MlTYO and tyramine (10 mM) as the substrate (Figure 3.2.2.4-1). As expected, the color of the reaction mixture turned brown after 4 h of reaction, and the coloration gradually became stronger with prolonged incubation time. In HPLC analysis, <1 mM 4HPAAld was detected during the reaction, whereas approximately 5 mM tyramine was consumed after 18 h of reaction. That is, much less 4HPAAld was produced than the amount of tyramine consumed, strongly suggesting that the brown compound was formed from 4HPAAld. By HPLC analysis, some shunt product peaks were detected, but we were unable to examine if the brown color was derived from these compounds because of their low yields (Figure 3.2.2.4-2).

MlTYO catalyzes the formation of 4HPAAld, NH_3, and H_2O_2 from tyramine and 1.92 ± 0.23 mM H_2O_2 was detected in the *in vitro* reaction using purified recombinant MlTYO and tyramine. Because H_2O_2 is a reactive compound, the brown compound might be formed from 4HPAAld by reaction with H_2O_2. To test this possibility, bovine liver catalase was added to the *in vitro* reaction mixture of purified recombinant MlTYO and tyramine (Figure. 3.2.2.4-1). As a result, the observed concentration of H_2O_2 decreased to 0.089 ± 0.003 mM at 24 h, and more tyramine was consumed than in the absence of catalase. However, the color of the reaction mixture still changed to dark-brown. Therefore, H_2O_2 was suggested to have no relationship with the formation of the brown compound.

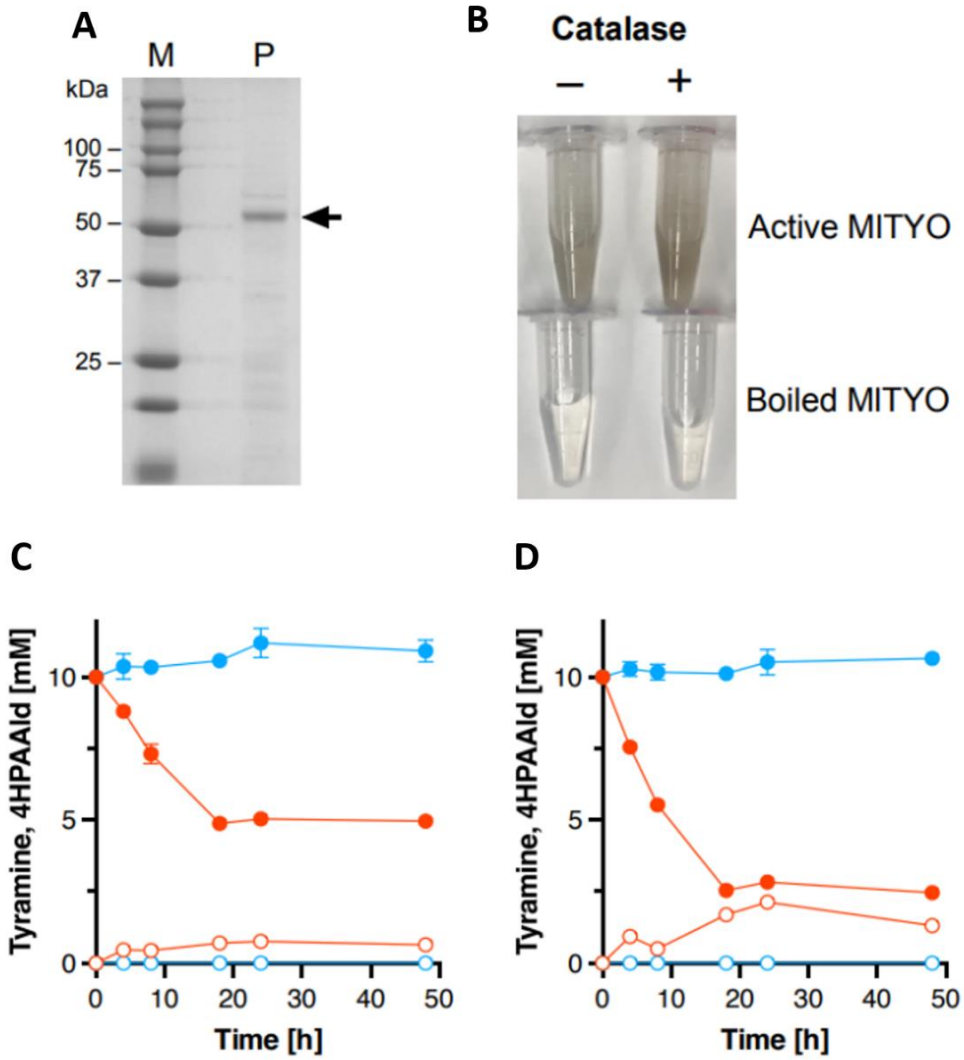

Figure 3.2.2.4-1. ***In vitro*** **assay of purified recombinant MlTYO with tyramine.**

(A) SDS–PAGE analysis of purified recombinant MlTYO (51.3 kDa). M, marker; P, purified protein (2 μg). **(B)** Photograph of the reaction mixtures with or without catalase at 24 h of reaction. Upper, active enzyme; lower, boiled enzyme. **(C, D)** Profiles of the reaction mixtures without catalase (C) and with catalase (D). Tyramine, solid circles; 4HPAAld, open circles; red, active enzyme; blue, boiled enzyme. Data are presented as mean values with standard deviations from three independent experiments.

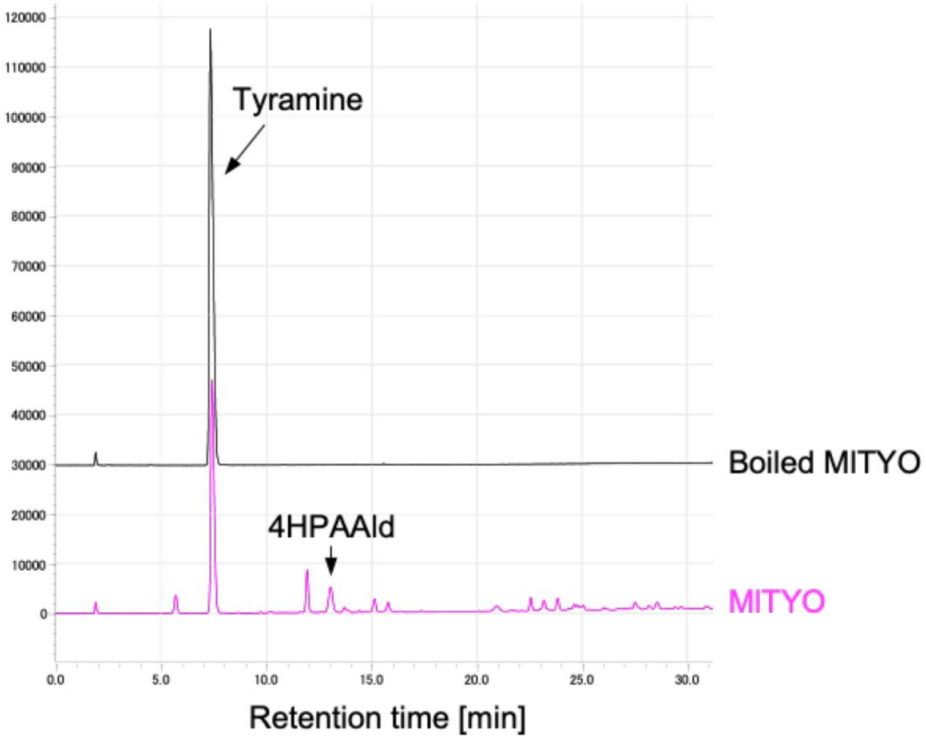

Figure 3.2.2.4-2. HPLC analysis of reaction mixtures of *in vitro* experiments with purified recombinant MlTYO and tyramine as a substrate.

In vitro reactions were conducted in solutions (1.0 mL) containing 200 mM potassium phosphate (pH 7.0), 10 mM tyramine-HCl, and 0.04 U purified MlTYO at 30°C. After samples collected at 24 h were boiled and centrifuged, the diluted supernatants were subjected to HPLC analysis, and the eluted compounds were detected by measuring the absorbance at 280 nm.

3.2.2.5 Optimization of tyrosol production

For high tyrosol production, 4HPAAld synthesized from tyramine catalyzed by MlTYO should be converted promptly to tyrosol catalyzed by a highly active ADH and/or AR (instead of endogenous reductase) before the formation of undesirable brown compound. To achieve this, the gene encoding *E. coli* YahK, which is a medium-chain dehydrogenase/reductase used for conversion of 4HPAAld to tyrosol **[16, 46]**, was integrated into the *pykA* locus of strain YDO under the control of the *T7* promoter. When the resulting strain YDOK was cultured in the same growth conditions as described above, tyrosol production was markedly enhanced to 11.0 ± 0.3 mM (1.52 g/L) after 24 h of cultivation (Figure 3.2.2.5-1A). However, even though tyramine was consumed from 24 to 48 h, the tyrosol production remained constant. The broth also turned dark-brown (Figure 3.2.2.5-1D). I therefore tried another approach to improve the tyrosol titer.

Glycerol was used to enhance the supply of NADH, which is required for the reactions catalyzed by DHPR and YahK **[34, 35]**. As shown in Figure. 3.2.2.5-1A, strain YDOK completely consumed glycerol by 24 h in medium containing 10 g/L glycerol, which indicated that further enhancement of NADH by increasing the concentration of glycerol was important. After increasing glycerol concentration to 20 or 40 g/L, almost no cell growth after 24 h was observed and that significant amount of tyramine was accumulated, suggesting that the lack of reducing power was a limited factor under this condition. Thus, the effect of glycerol concentration in the medium was examined (Figure. 3.2.2.5-1BC). When

40 g/L glycerol was added into the medium, the tyrosol yield increased to 17.5 ± 0.5 mM (2.42 g/L) after 72 h of cultivation, and no obvious color change was observed in the broth (Figure. 3.2.2.5-1CD). The tyrosol titer with 20 g/L glycerol was almost the same as that with 40 g/L glycerol. Considering that cell growth, glycerol consumption, and tyrosol yield were almost the same between the two conditions, viabilities of strain YDOK were perhaps lost after 48 h cultivation and NADH amount is sufficient to participate in the reactions. Thus, the glycerol concentration in the medium is an important factor for obtaining high tyrosol production.

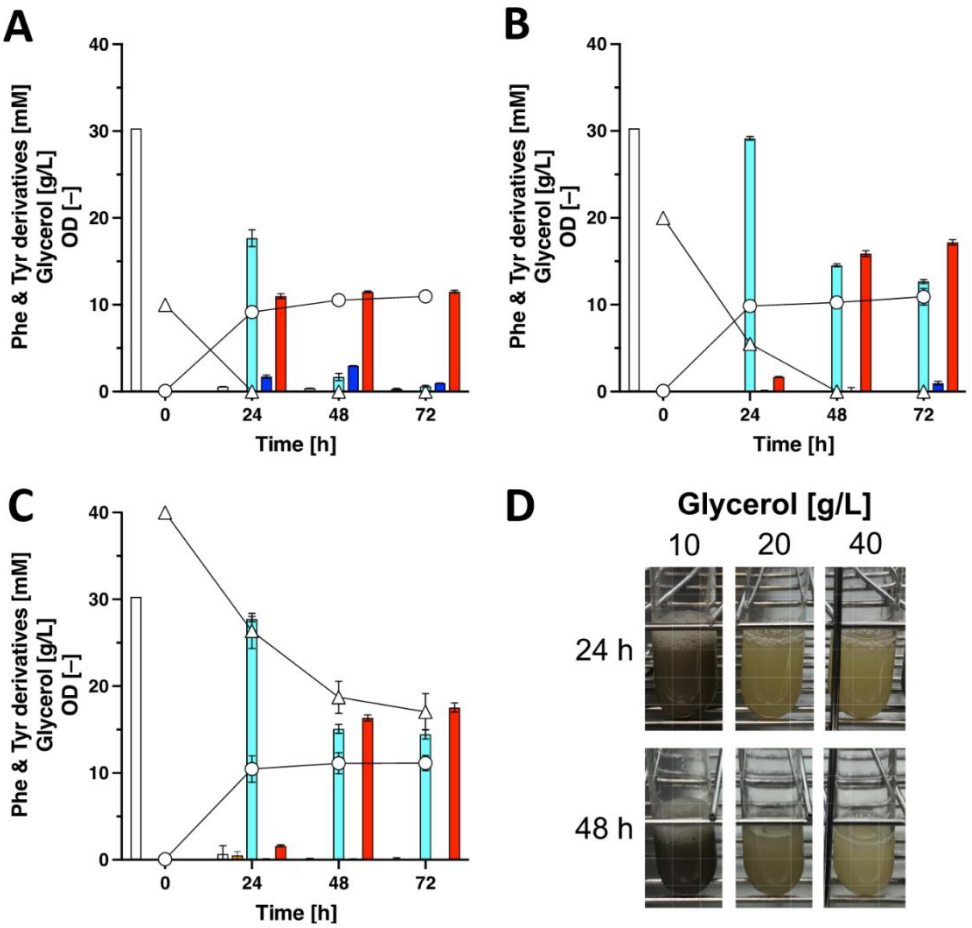

Figure 3.2.2.5-1. Tyrosol production by strain YDOK in media containing 10, 20, and 40 g/L glycerol, respectively.

(A–C) Strain YDOK was cultured in medium containing 10 **(A)**, 20 **(B)**, or 40 **(C)** g/L glycerol for 72 h at 30 °C, respectively. Phe, white bars; tyramine, light-blue bars; 4HPAAld, blue bars; tyrosol, red bars; OD, white circles; glycerol, white triangles. Data are presented as mean values with standard deviations from three independent experiments. **(D)** Photographs of culture broth of strain YDOK after 24 and 48 h of cultivation.

3.3 Discussion

In this chapter, I constructed Tyr- and tyrosol-producing strains by chromosomal engineering with *T7* promoter expression system. The plasmid-free Tyr-producing strain produced 28.6 ± 1.1 mM (5.19 g/L) Tyr. Then, the strain was applied for production of tyrosol by expressing selected TDC-, TYO-, and YahK-encoding genes under the control of *T7* promoter on the chromosome **[39]**. Finally, the titer of tyrosol was elevated to 17.5 mM (2.42 g/L) by eliminating bottleneck steps and increasing the glycerol concentration in the medium to 40 g/L. This titer is 1.5-fold that of the plasmid-based strain (11.5 mM, 1.58 g/L) **[30]**.

In addition to my platform, three other pathways have been constructed in *E. coli* and yeast; these are based on natural and non-natural biosynthesis pathways (Figure 3.3-1) **[16, 46–58]**. The pathways are characterized by different routes to supply the intermediate 4-hydroxyphenylacetaldehyde (4HPAAld), which is converted to tyrosol by alcohol dehydrogenase(s) (ADHs) and aldehyde reductase(s) (ARs). In the Ehrlich pathway of *S. cerevisiae*, 4HPAAld is synthesized from tyrosine (Tyr) via 4-hydroxyphenylpyruvate (4HPPyr) by aminotransferase (AT) and phenylpyruvate decarboxylase (PPDC). Chung *et al*. reported a process for direct conversion of Tyr to 4HPAAld using aromatic acetaldehyde synthase (AAS; the AAS pathway). Recently, the styrene degradation pathway of *Pseudomonas putida* was applied for tyrosol production. In this pathway, 4-coumarate derived from Tyr by tyrosine ammonia-lyase (TAL) was transformed to 4HPAAld by a cascade of reactions catalyzed by the enzymes

ferulate decarboxylase 1 (FDC1), styrene monooxygenase (SMO), and styrene oxide isomerase (SOI) (the SMO/SOI pathway). By comparison, the titer of strain YDOK is 4-times those of *E. coli* carrying the AAS and SMO/SOI pathways **[49, 50]** and comparable to the highest value (2.8 g/L) obtained via the Ehrlich pathway **[46].** Recently, Ruan *et al.* produced 21.8 g/L tyrosol from 50 g/L Tyr using a whole cell *E. coli* catalyst in flask-scale cultivation, but this still had the disadvantage of the need for the expensive material $NADP^+$ as a cofactor **[59]**. Thus, the TDC/TYO pathway has potential for application in industrial tyrosol production processes.

Higher glycerol concentration in the culture medium was effective in achieving high tyrosol production in strain YDOK (Figure 3.2.2.5-1). However, when >20 g/L glycerol was added, tyrosol production was delayed, although almost all the Phe was converted to tyramine by 24 h of cultivation, suggesting that a high glycerol concentration might inhibit MlTYO. To avoid retardation of tyrosol production, feeding control of glycerol may be effective. Protein engineering to modify MlTYO to release it from glycerol inhibition might also be effective.

Melanin, a naturally occurring brown-to-black pigment with complex structure, is produced by a variety of organisms, but not by *E. coli* **[60–62]**. It can be synthesized from Tyr by tyrosinase and 4HPPyr dioxygenase (Figure 3.3-2). The tyrosinase, a copper-dependent dioxygenase, catalyzes the formation of dopaquinone via DOPA as an intermediate. The dopaquinone is then converted

to melanin by a series of nonenzymatic reactions involving cyclization, oxidation, and polymerization. 4HPPyr dioxygenase converts 4HPPyr supplied by transamination of Tyr into 2,5-dihydroxyphenylacetate (homogentisate), which spontaneously oxidizes and polymerizes to produce melanin. In both routes, the dihydroxyphenol structure is important for melanogenesis. However, melanin-like pigment observed in this study was suggested to be formed from 4HPAAld, which has only one hydroxy group, showing the existence of a further route of melanogenesis.

My goal is the development of reliable microbial cell factories that produce a variety of industrially relevant Tyr-related chemicals from renewable biomass resources. This could be simply and rapidly achieved using strains constructed in this study. Especially, for industrial applications, chromosomal engineering has great advantages, and I succeeded in constructing a chromosomally engineered high-tyrosol-producing strain. In the near future, the system might also be applied in co-culture metabolic engineering with high-Phe producers that can use biomass as carbon source **[54, 63, 64]**.

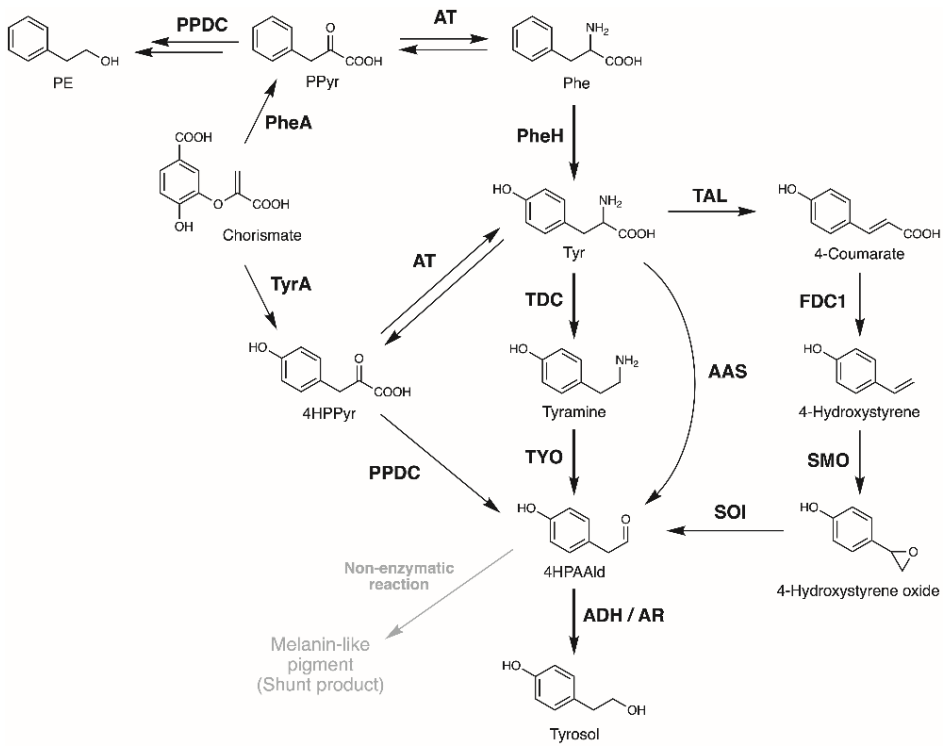

Figure 3.3-1. Tyrosol biosynthetic pathways.

Tyr (tyrosine); 4HPAAld (4-hydroxyphenylacetaldehyde); 4HPPyr (4-hydroxyphenylpyruvate); Phe (phenylalanine); PPyr (phenylpyruvate); PE (phenylethanol); PheH (Phe hydroxylase); TDC (Tyr decarboxylase); TYO (tyramine oxidase); ADH (alcohol dehydrogenase); AR (aldehyde reductase); AAS (aromatic acetaldehyde synthase); AT (aminotransferase); PPDC (PPyr decarboxylase); TAL (tyrosine ammonia-lyase); FDC1, (ferulate decarboxylase 1); SMO (styrene monooxygenase); SOI (styrene oxide isomerase); PheA (fused chorismate mutase/prephenate dehydratase); TyrA (fused chorismate mutase/prephenate dehydrogenase).

A

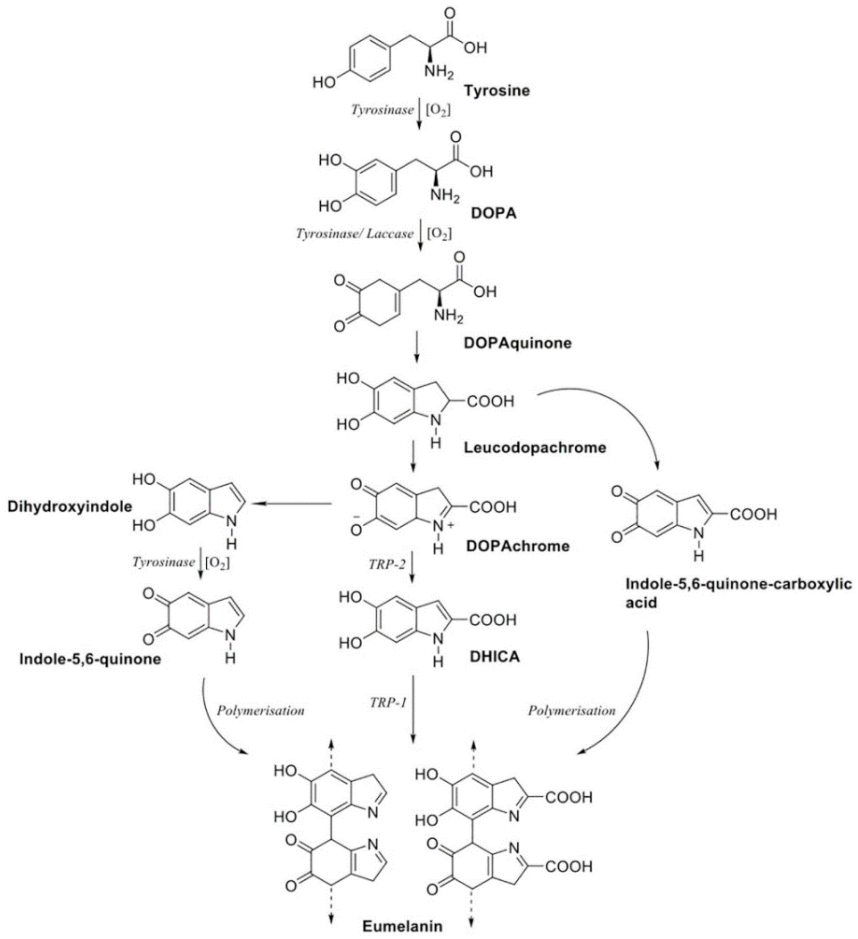

B

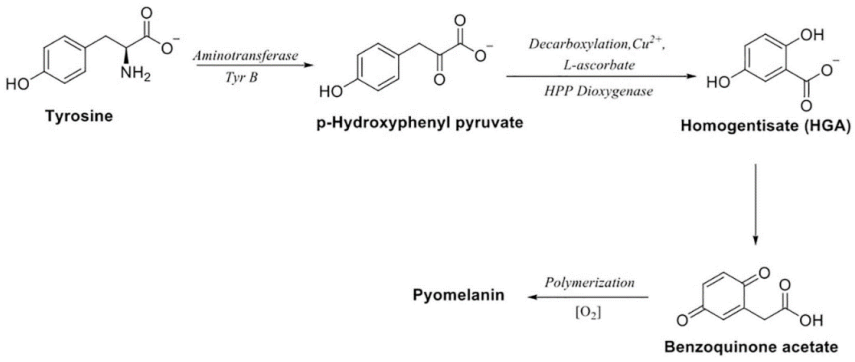

Figure 3.3-2. Biosynthesis of melanin from tyrosine by tyrosinase (A) and 4-hydroxyphenylpyruvate dioxygenase (B).

3.4 Material and methods

3.4.1 General

All media, chemicals, and reagents were of analytical grade and were purchased from FUJIFILM Wako Pure Chemical Corporation (Osaka, Japan), Sigma-Aldrich Japan K.K. (Tokyo, Japan), or Tokyo Chemical Industry Co., Ltd. (Tokyo, Japan). 4HPAAld was a product of Santa Cruz Biotechnology, Inc. (Dallas, TX, USA). PCR was performed using a GeneAmp PCR System 9700 thermal cycler (Thermo Fisher Scientific Inc., Waltham, MA, USA) with KOD DNA polymerase (Toyobo Co. Ltd., Osaka, Japan) according to the manufacturer's protocols. General genetic manipulations of *E. coli* were performed according to standard protocols. Protein concentrations were determined by the Bradford method with bovine serum albumin as the standard.

3.4.2 Strains and culture conditions

The *E. coli* JM109 (Nippon Gene Co., Ltd., Tokyo, Japan) was routinely used for plasmid construction. Engineered strains were generated from *E. coli* MG1655(DE3) via the Red-recombination method, flippase (FLP)/FLP recognition target (FRT) site-specific recombination, and P1 transduction. Briefly, the target genes amplified by PCR together with a Km-resistance marker were integrated into appropriate loci in the chromosome of *E. coli* MG1655(DE3) by Red-recombination, respectively. For pathway construction, the genes were

assembled step-by-step in appropriate hosts by P1 transduction along with recycling of the antibiotic marker by FLP/FRT site-specific recombination. In particular, *feaB*-deficiency, to prevent 4-hydroxyphenylacetate formation from 4HPAAld, is essential for effective tyrosol production. The knockout of *tyrB* is useful to prevent formation of 4HPPyr and PPyr from Tyr and Phe.

The growth medium used for pre-cultivation was LB broth medium, including 10 g/L NaCl, 10 g/L Hipolypeptone, and 5.00 g/L yeast extract (D-3H, Nihon Pharmaceutical, Tokyo, Japan). The tyrosol production used HCFY medium, which was consisted of 1%, 2%, 4% (w/v) glycerol as carbon source, 5.0 g/L dried-yeast extract, 5.0 g/L (30.3 mM) Phe, phosphate/citrate buffer including 13.3 g of KH_2PO_4, 4 g of $(NH_4)_2HPO_4$ and 1.7 g of citric acid, 1.2 g/L $MgSO_4$-$7H_2O$, 4.5 mg/L thiamin-HCl and trace metals including 100 mg of Fe(III) citrate, 2.5 mg of $CoCl_2 \cdot 6H_2O$, 15 mg of $MnCl_2 \cdot 4H_2O$, 1.5 mg of $CuCl_2 \cdot 2H_2O$, 3 mg of H_3BO_3, 2.5 mg of $Ma_2MoO_4 \cdot 2H_2O$, 13 mg of Zn acetate$\cdot 2H_2O$ and 8.4 mg of disodium dihydrogen ethylendiaminetetraacetate$\cdot 2H_2O$ (EDTA). Ampicillin (Ap), chloramphenicol (Cm), and streptomycin (Sm) were added to media at 100, 30, and 20 mg/L, respectively. Km was added to media at 25 mg/L to maintain plasmids. For the selection of gene knockout mutants, Km was used at 13 mg/L.

3.4.3 Plasmid construction

For constructing the plasmids, the standard procedures were carried out for polymerase chain reactions (PCR), DNA purifications, enzyme digestions, ligation reactions, and plasmid extractions. The PCR conditions were as follows: 98°C for 60 s, 98°C for 15 s, 58°C for 5 s, and 68°C for 5 s·kb-1 × n kb (n, length of gene fragment). The same strategy for all constructed plasmids with restriction sites was used in this work. All plasmids constructed and gene insertion in the chromosome of *E. coli* MG1655(DE3) were verified by sequencing.

3.4.4 Construction of tyrosol-producing platform by chromosomal engineering

For constructing the strain Y1, DNA fragment containing a modified Tyr-producing module and a Km-resistance marker flanked with FRT sites and 50-bp homology arms for *ascF* locus was obtained by PCR with pETDuet-FRT-PheH1-BH4R plasmid as the template and primers AscF-f (GACTGATAACAACTACATCTACCCT ACTGATAACAGGATAAAATCCGATGATTCCGGGGATCCGTCGACC) and AscF -r (ACTTTCTGGAAATACTGACATTTTCATCCTCAATTAAGACTTACTTCTTTA TTCGCCAATCCGGATATAG). *E. coli* MG1655(DE3) expressing Red recombinase was transformed with the amplicon and then Km-resistance strain was selected. Then, the Km marker in the obtained strain was removed by FLP recombinase. The gene integration and marker elimination were confirmed by PCR as shown below.

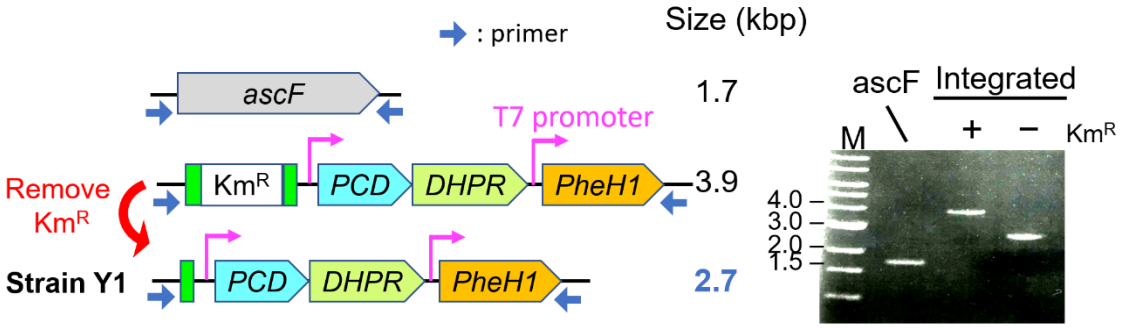
: primer
Size (kbp)
ascF
1.7
T7 promoter
Remove
KmR
KmR
PCD
DHPR
PheH1
3.9
Strain Y1
PCD
DHPR
PheH1
2.7
ascF
Integrated
M
+
−
KmR
4.0
3.0
2.0
1.5

For constructing strain Y2, each of GsPheH1, PCD, DHPR, and SKIK-tagged DHPR genes were integrated into *feaB* locus on the chromosome of strain Y1 by P1 transduction used appropriate *E. coli* MG1655(DE3) derivatives as donors. For integration of DNA fragments into *feaB* locus, primers feaB-f (TCGCTGCGTACACTGAAATCACACTGGGTAAATAATAAGGAAAAGTGATG ATTCCGGGGATCCGTCGACC) and feaB-r (TGCCGTTTTTTACTTATGAGCGAA CCAGATTAATACCGTACACACACCGAATTCGCCAATCCGGATATAG) were employed. The gene integration and marker elimination were confirmed by PCR as shown below.

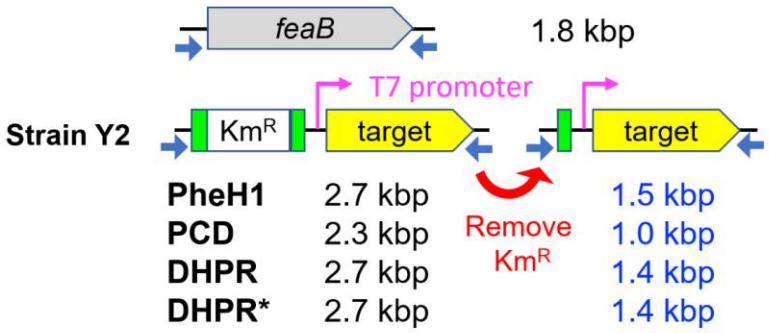

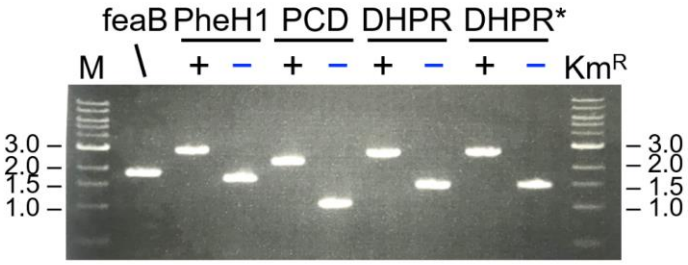

For constructing strain Y3, each of GsPheH1, PCD, and SKIK-tagged DHPR genes were integrated into *pflBA* locus on the chromosome of strain Y2 by P1 transduction used appropriate strains as donors. For integration of DNA fragments into *pflBA* locus, primers pflBA-f (CGAAGTACGCAGTAAATAAAAAATCCACTTAAG AAGGTAGGTGTTACATGATTCCGGGGATCCGTCGACC) and pflBA-r (CTCAAT AAAGTTGCCGCTTTACGGGGAAATTAGAACATTACCTTATGACCATTCGCCA ATCCGGATATAG) were used. The gene integration and marker elimination were confirmed by PCR as shown below.

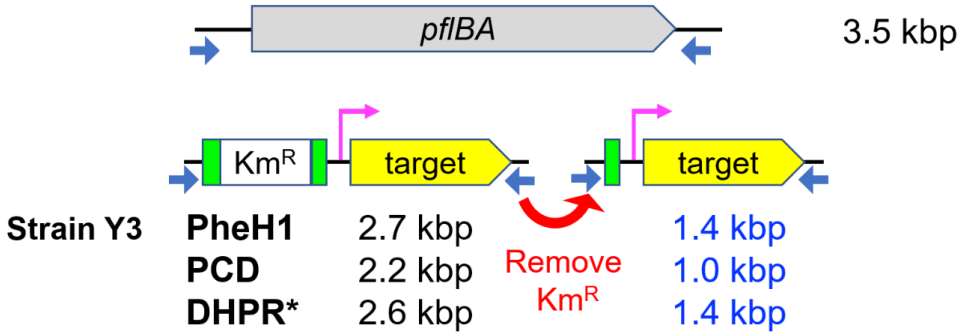

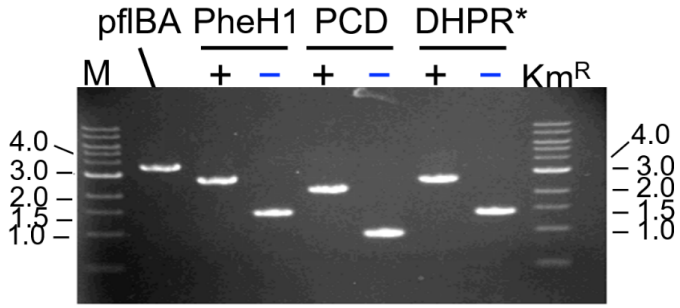

To obtain strain YD, YDO and YDOK, each of *TDC*, *MlTYO* and *YahK* genes was integrated into *tyrB*, *lacZ* and *pykA* loci, respectively. The primer pairs of Δ*tyrB*-F (GTTTATTGTGTTTTAACCACCTGCCCGTAAACCTGGAGAACCATCGCGTGA TTCCGGGGATCCGTCGACC) and Δ*tyrB*-R (GCTGGGTAGCTCCAGCCTGCTTT CCTGCATTACATCACCGCAGCAAACGCGGAAGCAGTGTGACCGTGTGCTTC TC), Δ*lacZ*-F (GTTGTGTGGAATTGTGAGCGGATAACAATTTCACACAGGAAA CAGCTATGATTCCGGGGATCCGTCGACC) and Δ*lacZ*-R (ACGGGCAGACATGG CCTGCCCGGTTATTATTATTTTTGACACCAGACCAACGGAAGCAGTGTGAC GTGTGCTTCTC), Δ*pykA*-FRT-F (TTTCATGTTCAAGCAACACCTGGTTGTTTC AGTCAACGGAGTATTACATGATTCCGGGGATCCGTCGACC) and Δ*pykA*-FRT-R (TGGCGTTTTCGCCGCATCCGGCAACGTACTTACTCTACCGTTAAAATACGA TTCGCCAATCCGGATATAG) were used to insert desired genes into the appropriate target loci. Amplified DNA fragments were treated with *DpnI*, purified by agarose-gel electrophoresis and NucleoSpin Gel and PCR Clean-up Kit (MACHEREY-NAGEL), and finally dissolved in sterilized pure water at a concentration of 5–10 ng/μl to obtain a linear DNA fragment solution. The gene integration and marker elimination were confirmed by PCR in the same manner of the development of the Tyr-producing strains as shown below.

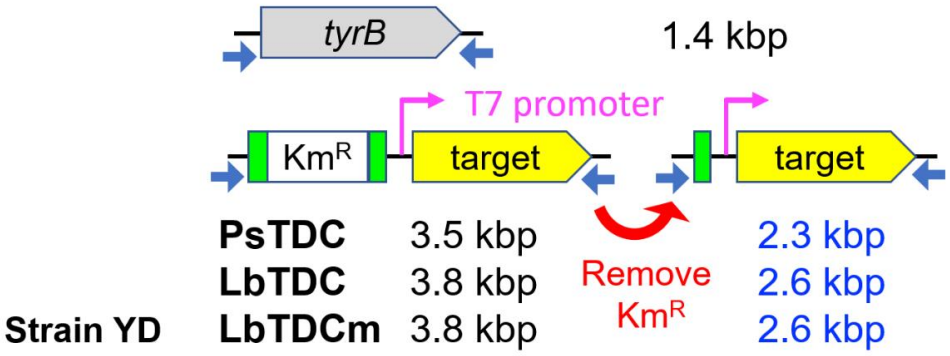
tyrB
1.4 kbp
T7 promoter
KmR
target
target
PsTDC 3.5 kbp
LbTDC 3.8 kbp
Strain YD LbTDCm 3.8 kbp
Remove KmR
2.3 kbp
2.6 kbp
2.6 kbp

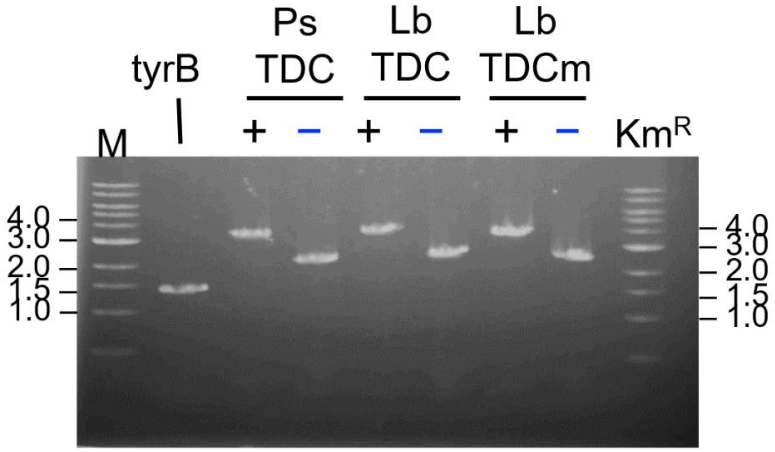
Ps TDC
Lb TDC
Lb TDCm
tyrB
M
+ − + − + −
KmR
4.0
3.0
2.0
1.5
1.0

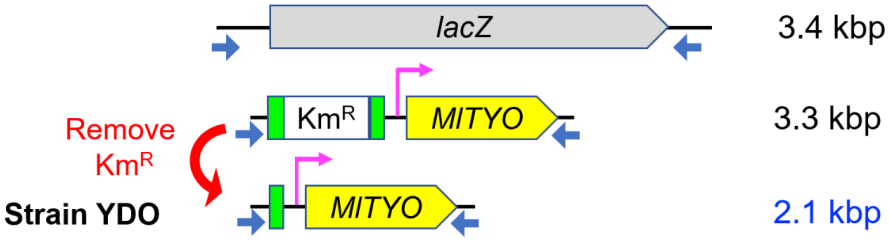
lacZ
3.4 kbp
KmR
MITYO
3.3 kbp
Remove KmR
Strain YDO
MITYO
2.1 kbp

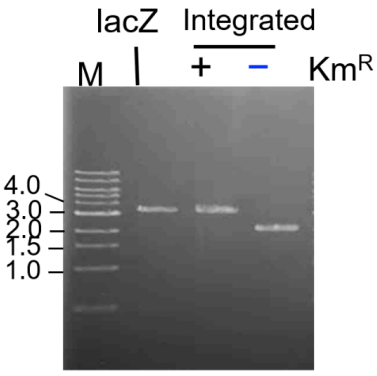
lacZ
Integrated
M
+ −
KmR
4.0
3.0
2.0
1.5
1.0

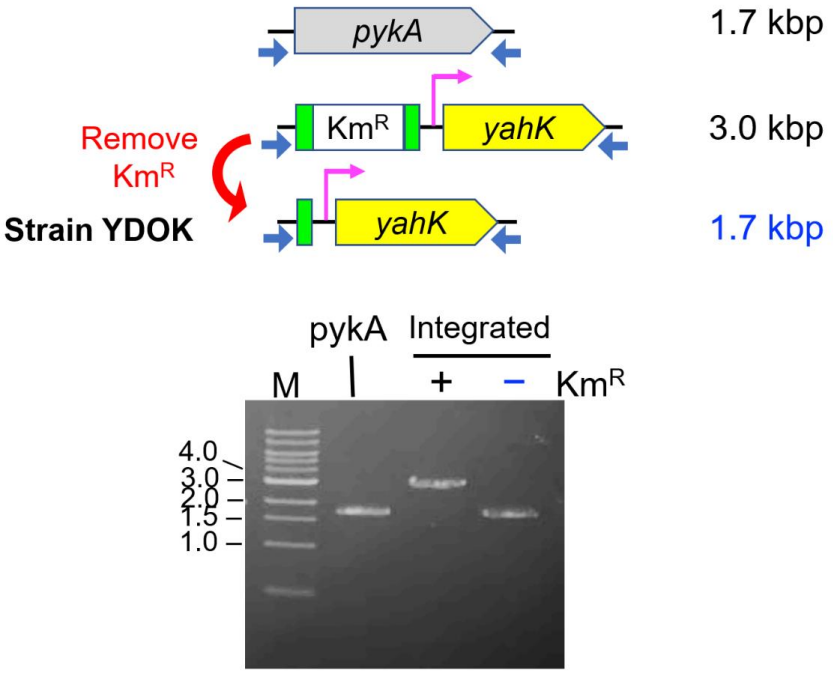

3.4.5 Elimination of the Km cassette by FLP/FRT recombination

The 100 μL overnight cultivated pre-culture was transplanted in 5 mL LB liquid medium with 13 mg/L Km, and cultured for about 1 h in a shaker at 30°C and 180 rpm until the OD_{600} became 0.3. Hereafter, centrifuging for 15,000 rpm and 1 minute at 4°C, discarding the supernatant, washing for three times with 1 mL ice chilled sterilized milli Q water, and dissolved in 30 μL of the ice chilled sterilized milli Q water after the third centrifugation. The key for excision of the Km cassette was a yeast FLP and flippase recognition target (FRT) site, and a strain harboring an FRT-Km-FRT cassette was transformed with pCP20 encoding the FLP gene, and then the transformant was cultivated at 30°C overnight on Chloramphenicol (Cm)–LB agar plates (Cm, 15 μg/mL). The pCP20 plasmid can express the flippase recombination enzyme (FLP) gene under

30°C, so that one FRT site and the Km resistance gene can be eliminated. Colonies grown on solid media were used for streaking at 42°C or 37°C overnight, and several colonies were randomly selected to check their growth on LB, Cm–LB, and Km–LB agar plates. Because of the temperature sensitivity of pCP20, cultivating the strain carrying pCP20 at 42°C or 37°C can eliminate pCP20 and obtain a non-resistant strain. A positive selecting result is that strains only grow on LB plates.

3.4.6 Transfer of an inserted section of chromosome by P1 transduction

The *E. coli* strain harboring an FRT-Km-FRT cassette and an inserted desired gene in a target locus of chromosome was used as a donor strain. Using sterilized toothpicks to take the donor strains, which grown on the LB solid plates with Km resistance and inoculated them into test tubes containing 5 mL of liquid LB medium. After culturing in a shaker at 37°C and 180 rpm rotating speed until the culture was slightly turbid, adding 50 μL of sterilized 1 M $CaCl_2$ and 200 μL of the prepared *E. coli* W3110 P1 phage solution to the test tubes step by step. Continuously, cultivating the test tubes in the shaker with the same conditions until the bacteria dissolved and filaments appeared. Afterwards, adding chloroform 20 μL and cultivating in the shaker for 5 minutes. For subsequent application and storage, the supernatant obtained after centrifugation at 15,000 rpm for 5-10 minutes was filtered with a pore size of 0.2 μm filtration sterilization devices and stored at 4°C.

A Km-sensitive *E. coli* strain was used as a recipient strain. As the first step in infecting the accepter strain with the prepared phage solution, the donor strain was grown in Km–LB medium at 37°C to an OD_{660} of 0.1. Then, 50 µL of the cold sterilized 1 M $CaCl_2$ was added into the 5 mL culture. The prepared *E. coli* W3110 P1 lysate 20 µL and 200 µL above culture were transferred to a 2 mL-tube, then the mixture was incubated at 37°C for 20 minutes. After incubation, 100 µL of sterilized 1 M trisodium citrate and 700 µL of LB medium were added to the cell solution, and it was then incubated at 37°C and stood for 40 minutes. 200 µL of the solution were spread onto Km–LB agar, and the cells were then cultivated at 37°C overnight. Several Km-resistant strains were picked and checked by colony-direct PCR.

3.4.7 Production of tyrosine and tyrosol

E. coli MG1655 derivatives were pre-cultured in 5 mL of LB medium at 30°C for 16 h with reciprocal shaking at 250 rpm. The aliquots of the cultures were inoculated into 5 mL of HCFY medium containing 5.00 g/L (30.3 mM) Phe, and cultivated at 30°C with 250 rpm shaking. To induce protein expression, IPTG was added to a final concentration of 500 µM at 4 h of cultivation. 500 µL of samples were collected at appropriate time-points and analyzed by HPLC. Optical density (OD) measurements at 660 nm were also taken using a NanoDrop 2000C spectrophotometer (Thermo Fisher Scientific), using cuvettes after dilution in a 1 M HCl solution to dissolve Tyr. Glycerol concentration was analyzed by an enzymatic method using the F-kit (R-Biopharm AG, Darmstadt,

Germany).

3.4.8 HPLC analysis

After culture aliquots diluted with 1 M HCl were centrifuged, the supernatants (10 μL) were analyzed using an HPLC system (Shimadzu Co., Kyoto, Japan), equipped with a COSMOSIL 5C18-MS-II column (column length, 150 mm; inner diameter, 3.0 mm; particle size, 5 μm; Nacalai Tesque, Inc., Kyoto, Japan). Buffer A [0.1% (v/v) trifluoroacetic acid solution] and buffer B [methanol with 0.1% (v/v) trifluoroacetic acid] were used as the mobile phases, and compounds were eluted at 40°C and a flow-rate of 0.4 mL/min, with increasing concentrations of buffer B as follows: 2%, 0−2 min; 2%–80% (linear gradient), 2–35 min. Eluted compounds were detected by measuring absorbance at 210 and 280 nm.

3.4.9 Preparation of crude cell extracts containing TDC or TYO

For the preparation of the crude extracts, *E. coli* MG1655(DE3) harboring the *TDC* or *TYO* gene was pre-cultivated in 2.5 mL LB medium at 30°C overnight. The pre-culture was inoculated into 150 mL LB medium in scale conical flasks to OD_{600} reached 0.2. Then, the strain continued to be cultivated at 30°C until the OD_{600} reached to 1, and 0.5 mM IPTG was added for 4 h cultivation at 30°C. Subsequently, cells were harvested from 150 mL of culture by centrifugation at 20,000 × g at 4°C for 30 minutes, and washed three times with 20 mL of 50 mM ice chilled phosphate buffer (PSB,

KH_2PO_4 with KOH for pH adjustment, pH 8.0). Before adding the PSB for the third time washing, measuring the OD_{660} once, and unifying the OD_{660} to 100 by adjusting the dissolved amount of PSB. The cells were disrupted by sonication (BRANSON) on ice and centrifuged at 15,000 rpm for 30 min at 4°C. The supernatant was used as cell-free extracts (CFE) for enzyme screenings *in vitro* assays. The protein concentration of the CFE was measured using Protein Assay Bradford reagent (FujiFilm wako Pure chemical corporation) with bovine serum albumin (BSA) as a standard. The whole cells, soluble and insoluble fragments were also subjected to SDS-PAGE analysis. The proteins were visualized by staining with 2 × SDS Sample buffer (0.125 M Tris-HCl buffer, 10%(v/v) 2-mercaptoethanol, 4% (w/v) $CH_3(CH_2)_{11}OSO_3Na$, 10% (w/v) sucrose, 0.01% (w/v) bromophenol blue).

3.4.10 *In vitro* assay for TDC activity

In vitro assay was conducted in solution (1 mL) containing 1 mM Tyr, cofactor 100 μM pyridoxal phosphate (PLP), and 400 μg prepared crude cell lysate in 40 mM Tris–HCl (pH 7.0) or 160 mM sodium acetate [pH 5.0, the optimal pH for *Lactobacillus brevis* TDC mutant (LbTDCm)] buffer at 30°C for up to 90 min. After samples (100 μL) collected at 0, 5, 10, 20, 30, 40, 60, and 90 min were boiled and centrifuged, the supernatant was subjected to HPLC analysis. Initial reaction velocity was calculated for the linear portion of the reaction (up to 20 min), and one unit (U) was defined as the amount of enzyme that catalyzed the formation of 1 μmol of tyramine per minute.

3.4.11 *In vitro* assay for TYO activity

In vitro assay was performed in solution (1 mL) containing 1 mM tyramine-HCl,1 mM ascorbate, and 400 μg crude cell lysate in 50 mM potassium phosphate buffer (pH 7.0) at 30°C for up to 90 minutes. Alternatively, instead of the crude lysate, an appropriate amount of purified recombinant MlTYO was added to determine the activity. After samples (100 μL) collected at 0, 5, 10, 20, 30, 40, 60, and 90 minutes were boiled and centrifuged, the supernatant was subjected to HPLC analysis. Initial velocity was calculated for the linear portion of the reaction (up to 30 minutes), and one U was defined as the amount of enzyme that catalyzed the formation of 1 μmol of 4HPAAld per minute.

3.4.12 *In vitro* assay of the purified MlTYO

To confirm that the black brown compound was formed from 4HPAAld, the purified MlTYO was prepared as follows. MlTYO was expressed and purified as a His-tagged recombinant protein. A DNA fragment was prepared by PCR using primers 5′-AGATATACATATGAGCAACCCGCATGTCGTGATCG-3′ and 5′-CGGAAGCAGTGTGACCGTGTGCTTCTC-3′, pCF1s-MlTYO as the template, and was cloned into the *Nde*I and *Xho*I sites of vector pColdI (Takara Bio Inc., Shiga, Japan). Then, liquid culture of *E. coli* JM109 harboring the constructed plasmid in LB with Ap at 37°C was induced by adding 500 μM IPTG when the OD at 600 nm reached approximately 0.5. The cultivation was continued for an additional 20 h at 16°C. After the cells were harvested and washed once with

chilled buffer C (20 mM sodium phosphate, 500 mM NaCl; pH 7.4) including 20 mM imidazole, they were suspended in 20 mL of the same buffer and disrupted by sonication. The purification of recombinant His-tagged MlTYO protein was carried out using an ÄKTAexplorer 10S system (GE Healthcare Japan Co., Tokyo, Japan) equipped with a HiTrap IMAC HP column (1 mL) charged with Ni^{2+} ions (GE Healthcare Japan). Buffer C and buffer D (20 mM sodium phosphate, 500 mM NaCl, 500 mM imidazole; pH 7.4) were used as the mobile phase, and protein was eluted at a flow-rate of 1.0 mL/min, with increasing concentrations of buffer D as follows: 4%, 0−2 min; 4%–100% (linear gradient), 2–21 min. Eluted protein was monitored by measuring absorbance at 280 nm. After the fractions containing MlTYO were confirmed by sodium dodecyl sulfate–polyacrylamide gel electrophoresis (SDS–PAGE) analysis, they were dialyzed against 50 mM potassium phosphate buffer (pH 7.0) at 4°C and then concentrated by using an Amicon Ultra 10kDa (Merck). The enzyme purity was checked by SDS–PAGE.

In vitro reactions were conducted in solutions (1 mL) containing 200 mM potassium phosphate buffer (pH 7.0), 10 mM tyramine-HCl, and 0.04 U recombinant MlTYO with or without 135 U catalase (bovine liver, Tokyo Chemical Industry) at 30°C for 48 h. After 50 µL aliquots was collected at appropriate time points, they were boiled and centrifuged. The diluted supernatant was subjected to HPLC analysis as described above. Hydrogen peroxide formed was detected using a Pierce Quantitative Peroxide Assay Kit

(Thermo Fisher Scientific).

Chapter 4

Conclusion

In this study, I developed simple and convenient *E. coli* platforms for production of Tyr, which employ *Gulbenkiania* sp. PheH and a human BH4-regeneration system using endogenous MH4 as a cofactor by plasmid-based and chromosome-integrated methods. The Tyr titer of the plasmid-based engineered strain was 25.5 mM (4.63 g/L) in a medium supplemented with 30.3 mM (5.00 g/L) Phe with a test tube. The strains were successfully used to produce industrially attractive compound, tyrosol, with a yield of 1.58 g/L by installing a tyrosol-producing module consisting of genes encoding Tyr decarboxylase and tyramine oxidase on a plasmid.

Chromosomal engineering of *E. coli* has an advantage over the use of plasmids because it increases genetic stability without antibiotic feeding to the culture media and relieves the metabolic burden associated with plasmid maintenance. In addition, it enables flexible pathway engineering because more plasmids carrying artificial pathway genes are acceptable. Therefore, in my laboratory, plasmid-free Tyr-producing platform *E. coli* strains was previously constructed with *lac/tac* promoter-controlled *Gulbenkiania* sp. *PheH1* and BH4-regeneration-related genes, both of which were integrated into the five different loci of chromosome to make strain GsBR5. However, the strain produced small amounts of Tyr (3.23 ± 0.09 mM (0.586 g/L)) after 48 h. Therefore, I constructed a Tyr producing platform strain by integration of multiple *T7* promoter-controlled genes encoding PheH1, PCD, and SKIK-tagged DHPR on different chromosome loci (strainY3). The strain produced 28.6 ± 1.1 mM Tyr (5.19 g/L; 94.4% conversion from Phe). Then, I developed a tyrosol-producing platform from strain Y3 by expressing selected tyrosine decarboxylase-, tyramine oxidase (TYO)-, and medium-chain dehydrogenase/reductase (YahK)-encoding genes, all of

which were controlled by *T7* promoter and integrated into the chromosome. However, the strain produced a melanin-like pigment as a byproduct, which is suggested to be formed from 4-hydroxyphenylacetaldehyde (a TYO product/YahK substrate). By using a culture medium containing a high concentration of glycerol, which was reported to enhance NADH supply required for YahK activity, the final titer of tyrosol reached 2.42 g/L in test tube-scale cultivation with a concomitant decrease in the amount of pigment.

In conclusion, I developed *E. coli* platforms for production of Tyr and Tyr-related compound from Phe at multi-gram-per-liter levels in test-tube cultivation by plasmid-based and chromosome-engineered methods. The platforms would be useful for practical production of Tyr-derivatives at multi-grams-per-liter levels.

References

1. **Averesch, N. J. H., Krömer, J. O.:** Metabolic engineering of the shikimate pathway for production of aromatics and derived compounds–present and future strain construction strategies, Front. Bioeng. Biotechnol., **6**, 32 (2018).
2. **Cao M, Gao M, Suástegui M, Mei Y, Shao Z.:** Building microbial factories for the production of aromatic amino acid pathway derivatives: from commodity chemicals to plant-sourced natural products, Metab. Eng., **58**, 94–132 (2020).
3. **Thompson, B., Machas, M., Nielsen, D. R.:** Creating pathways towards aromatic building blocks and fine chemicals, Curr. Opin. Biotechnol., **36**, 1–7 (2015).
4. **Shen, Y. P., Niu, F. X., Yan, Z. B., Fong, L. S., Huang, Y. B., Liu, J. Z.:** Recent advances in metabolically engineered microorganisms for the production of aromatic chemicals derived from aromatic amino acids, Front. Bioeng. Biotechnol., **8,** 407 (2020).
5. **Yang D, Park SY, Park YS, Eun H, Lee SY.:** Metabolic engineering of *Escherichia coli* for natural product biosynthesis, Trends Biotechnol., **38**, 745–765 (2020).
6. **Robinson, C. J., Carbonell, P., Jervis, A. J., Yan, C., Hollywood, K. A., Dunstan, M. S., Currin, A., Swainston, N., Spiess, R., Taylor, S., and other 13 authors:** Rapid prototyping of microbial production strains for the biomanufacture of potential materials monomers. Metab. Eng., **60,** 168–182 (2020).
7. **Nielsen, J., Tillegreen, C. B., Petranovic, D.:** Innovation trends in industrial biotechnology, Trends Biotechnol., **40**, 1160–1172 (2022).

8. **Keasling, J., Garcia Martin, H., Lee, T. S., Mukhopadhyay, A., Singer, S. W., Sundstrom, E.:** Microbial production of advanced biofuels, Nat. Rev. Microbiol., **19**, 701–715 (2021).
9. **Xu, X., Liu, Y., Du, G., Ledesma-Amaro, R., Liu, L.:** Microbial chassis development for natural product biosynthesis, Trends Biotechnol., **38**, 779–796 (2020).
10. **Choi, K. R., Jang, W. D., Yang, D., Cho, J. S., Park, D., Lee, S. Y.:** Systems metabolic engineering strategies: integrating systems and synthetic biology with metabolic engineering, Trends Biotechnol., **37**, 817–837 (2019).
11. **Ko, Y. S., Kim, J. W., Lee, J.A, Han. T., Kim, G. B., Park, J. E., Lee, S. Y.:** Tools and strategies of systems metabolic engineering for the development of microbial cell factories for chemical production, Chem. Soc. Rev., **49**, 4615–4636 (2020).
12. **Rodriguez, A., Martínez, J. A., Flores, N., Escalante, A., Gosset, G., Bolivar, F.:** Engineering *Escherichia coli* to overproduce aromatic amino acids and derived compounds, Microb. Cell. Fact., **13**, 126 (2014).
13. **Zimmer, A., Mueller, R., Wehsling, M., Schnellbaecher, A., von Hagen, J.:** Improvement and simplification of fed-batch bioprocesses with a highly soluble phosphotyrosine sodium salt, J. Biotechnol., **186**, 110–118 (2014).
14. **Juminaga, D., Baidoo, E. E., Redding-Johanson, A. M., Batth, T. S., Burd, H., Mukhopadhyay, A., Petzold, C. J., and Keasling, J. D.:** Modular engineering of

L-tyrosine production in *Escherichia coli*, Appl. Environ. Microbiol., **78**, 89–98 (2012).

15. **Kim, S. C., Min, B. E., Hwang, H.G., Seo, S. W., Jung, G. Y.:** Pathway optimization by re-design of untranslated regions for L-tyrosine production in *Escherichia coli*, Sci. Rep., **5**, 13853 (2015).
16. **Koma, D., Kishida, T., Yoshida, E., Ohashi, H., Yamanaka, H., Moriyoshi, K., Nagamori, E., Ohmoto, T.:** Chromosome engineering to generate plasmid-free phenylalanine- and tyrosine-overproducing *Escherichia coli* strains that can be applied in the generation of aromatic-compound-producing bacteria, Appl. Environ. Microbiol., **86**, e00525-20 (2020).
17. **Daubner, S. C., Hillas, P. J., Fitzpatrick, P. F.:** Characterization of chimeric pterindependent hydroxylases: contributions of the regulatory domains of tyrosine and phenylalanine hydroxylase to substrate specificity, Biochemistry, **36,** 11574–11582 (1997).
18. **Flydal, M. I., Martinez, A.:** Phenylalanine hydroxylase: function, structure, and regulation, IUBMB Life., **65**, 341–349 (2013).
19. **Onishi, A., Liotta, L. J., Benkovic, S. J.:** Cloning and expression of *Chromobacterium violaceum* phenylalanine hydroxylase in *Escherichia coli* and comparison of amino acid sequence with mammalian aromatic amino acid hydroxylases, J. Biol. Chem., **266,** 18454–18459 (1991).

20. **Pribat A, Blaby IK, Lara-Núñez A, Gregory JF 3rd, de Crécy-Lagard V, Hanson AD.:** FolX and FolM are essential for tetrahydromonapterin synthesis in *Escherichia coli* and *Pseudomonas aeruginosa*, J. Bacteriol., **192**, 475–482 (2010).

21. **Satoh, Y., Tajima, K., Munekata, M., Keasling, J. D., Lee, T. S.:** Engineering of L-tyrosine oxidation in *Escherichia coli* and microbial production of hydroxytyrosol, Metab. Eng., **14**, 603–610 (2012).

22. **St-Laurent-Thibault, C., Arseneault, M., Longpré, F., Ramassamy, C.:** Tyrosol and hydroxytyrosol two main components of olive oil, protect N2a cells against amyloid-β-induced toxicity. Involvement of the NF-*κ*B signaling, Curr. Alzheimer Res., **8,** 543−551 (2011).

23. **Di Benedetto, R., Varì, R., Scazzocchio, B., Filesi, C., Santangelo, C., Giovannini, C., Matarrese, P., D'Archivio, M., Masella, R.:** Tyrosol, the major extra virgin olive oil compound, restored intracellular antioxidant defences in spite of its weak antioxidative effectiveness, Nutr. Metab. Cardiovasc. Dis., **17**, 535−545 (2007).

24. **Dudley, J. I., Lekli, I., Mukherjee, S., Das, M., Bertelli, A. A., Das, D. K.:** Does white wine qualify for french paradox? Comparison of the cardioprotective effects of red and white wines and their constituents: resveratrol, tyrosol, and hydroxytyrosol, J. Agric. Food Chem., **56**, 9362−9373 (2008).

25. **Chung, D., Kim, S. Y., Ahn, J.-H.:** Production of three phenylethanoids, tyrosol, hydroxytyrosol, and salidroside, using plant genes expressing in *Escherichia coli*, Sci. Rep., 72578 (2017).

26. **Ippolito, R. M., Vigmond, S.:** Process for preparing substituted phenol ethers via oxazolidine-structure intermediates, U.S. Patent US4760182 (1988).

27. **Yoo, S. E.:** Antihypertensive polyhalohydroxyisopropyl phenylalka(e)noic acid esters of alkylamino hydroxypropyloxyphenylalkyl alcohols, U.S. Patent US4450172 (1984).

28. **Borchard, U.:** Pharmacological properties of β-adrenoceptor blocking drugs, J. Clin. Basic Cardiol., **1**, 5−9 (1998).

29. **Granado, L., Tavernier, R., Henry, S., Auke, R. O., Foyer, G., David, G, Caillol, S.:** Toward sustainable phenolic thermosets with high thermal performances, ACS Sustain. Chem. Eng., **7**, 7209–7217 (2019).

30. **Satoh, Y., Fukui, K., Koma, D., Shen, N., Lee, T. S.:** Engineered *Escherichia coli* platforms for tyrosine-derivative production from phenylalanine using phenylalanine hydroxylase and tetrahydrobiopterin-regeneration system, Biotechnol. Biofuels Bioprod., **16**, 115 (2023).

31. **Satoh, Y., Tajima, K., Munekata, M., Keasling, J. D., Lee, T. S.:** Engineering of a tyrosol-producing pathway, utilizing simple sugar and the central metabolic tyrosine, in *Escherichia coli*, J. Agric. Food Chem., **60**, 979–984 (2012).

32. **Baba, T., Ara, T., Hasegawa, M., Takai, Y., Okumura, Y., Baba, M., Datsenko, K. A., Tomita, M., Wanner, B. L., Mori, H.:** Construction of *Escherichia coli* K-12 in frame, single-gene knockout mutants: the Keio collection, Mol. Syst. Biol., **2**, 0008 (2006).

33. **Daubner, S. C., Melendez, J., Fitzpatrick, P. F.:** Reversing the substrate specificities of phenylalanine and tyrosine hydroxylase: aspartate of tyrosine hydroxylase is essential for L-DOPA formation, Biochemistry, **39**, 9652–9661 (2000).

34. **da Silva, G. P., Mack, M., and Contiero, J.:** Glycerol: a promising and abundant carbon source for industrial microbiology, Biotechnol. Adv., **27**, 30–39 (2009).

35. **Wu, H., Karanjikar, M., and San, K. Y.:** Metabolic engineering of *Escherichia coli* for efficient free fatty acid production from glycerol, Metab. Eng., **25,** 82–91. (2014).

36. **Santos, C. N. S., Regitsky, D. D., Yoshikuni, Y.:** Implementation of stable and complex biological systems through recombinase-assisted genome engineering, Nat. Commun., **4**, 2503 (2013).

37. **Koma, D., Yoshida, E., Yamanaka, H., Moriyoshi, K., Keasling, J. D., Lee, T. S., and Ohmoto, T.:** *Escherichia coli* chromosomal engineering toward high titer phenylalanine and tyrosine production, Proc. Metab. Eng., **11**, 35–36 (2016).

38. **Koma, D., Yamanaka, H., Moriyoshi, K., Ohmoto, T., and Sakai, K.:** A convenient method for multiple insertions of desired genes into target loci on the *Escherichia coli* chromosome, Appl. Microbiol. Biotechnol., **93**, 815–829 (2012).

39. **Ning Shen, Yasuharu Satoh, Daisuke Koma, Hiroyuki Ohashi, Yasushi Ogasawara, Tohru Dairi.:** Optimization of tyrosol-producing pathway with tyrosine decarboxylase and tyramine oxidase in high-tyrosine-producing

Escherichia coli, J. Biosci. Bioeng., in press.

40. **Ojima-Kato, T., Nagai, S., and Nakano, H.:** *N*-terminal SKIK peptide tag markedly improves expression of difficult-to-express proteins in *Escherichia coli* and *Saccharomyces cerevisiae*, J. Biosci. Bioeng., **123**, 540–546 (2017).
41. **Koma, D., Fujisawa, M., Ohashi, H., Yamanaka, H., Moriyoshi, K., Nagamori, E., and Ohmoto, T.:** Production of 3-hydroxytyrosol from glucose by chromosomally engineered *Escherichia coli* by fed-batch cultivation in a jar fermenter, J. Agric. Food Chem., **71**, 9451–9459 (2023).
42. **Zhang, K. and Ni, Y.:** Tyrosine decarboxylase from *Lactobacillus brevis*: soluble expression and characterization, Protein Expr. Purif., **94**, 33–39 (2014).
43. **Zhu, H., Xu, G., Zhang, K., Kong, X., Han, R., Zhou, J., and Ni, Y.:** Crystal structure of tyrosine decarboxylase and identification of key residues involved in conformational swing and substrate binding, Sci. Rep., **6**, 27779 (2016).
44. **Roh, J. H., Suzuki, H., Azakami, H., Yamashita, M., Murooka, Y., and Kumagai, H.:** Purification, characterization, and crystallization of monoamine oxidase from *Escherichia coli* K-12, Biosci. Biotechnol. Biochem., **58**, 1652–1656 (1994).
45. **Alonso-Gutierrez, J., Koma, D., Hu, Q., Yang, Y., Chan, L. J. G., Petzold, C. J., Adams, P. D., Vickers, C. E., Nielsen, L. K., Keasling, J. D., and Lee, T. S.:** Toward industrial production of isoprenoids in *Escherichia coli*: lessons learned from CRISPR-Cas9 based optimization of a chromosomally integrated mevalonate pathway, Biotechnol. Bioeng., **115**, 1000–1013 (2018).

46. **Koma, D., Yamanaka, H., Moriyoshi, K., Ohmoto, T., and Sakai, K.:** Production of aromatic compounds by metabolically engineered *Escherichia coli* with an expanded shikimate pathway, Appl. Environ. Microbiol., **78**, 6203–6216 (2012).

47. **Sentheshanmuganathan, S. and Elsden, S. R.:** The mechanism of the formation of tyrosol by *Saccharomyces cerevisiae*, Biochem. J., **69**, 210–218 (1958).

48. **Hazelwood, L. A., Daran, J. M., van Maris, A. J. A., Pronk, J. T., and Dickinson, J. R.:** The Ehrlich pathway for fusel alcohol production: a century of research on *Saccharomyces cerevisiae* metabolism, Appl. Environ. Microbiol., **74**, 2259–2266 (2008).

49. **Chung, D., Kim, S. Y., and Ahn, J. H.:** Production of three phenylethanoids, tyrosol, hydroxytyrosol, and salidroside, using plant genes expressing in *Escherichia coli*, Sci. Rep., **7**, 2578 (2017).

50. **Lai, Y., Chen, H., Liu, L., Fu, B., Wu, P., Li, W., Hu, J., and Yuan, J.:** Engineering a synthetic pathway for tyrosol synthesis in *Escherichia coli*, ACS Synth. Biol., **11**, 441–447 (2022).

51. **Guo, W., Huang, Q., Liu, H., Hou, S., Niu, S., Jiang, Y., Bao, X., Shen, Y., and Fang, X.:** Rational engineering of chorismate-related pathways in *Saccharomyces cerevisiae* for improving tyrosol production, Front. Bioeng. Biotechnol., **7**, 152 (2019).

52. **Jiang, J., Yin, H., Wang, S., Zhuang, Y., Liu, S., Liu, T., and Ma, Y.:** Metabolic engineering of *Saccharomyces cerevisiae* for high-level production of salidroside

from glucose, J. Agric. Food Chem., **66**, 4431–4438 (2018).

53. **Li, X., Chen, Z., Wu, Y., Yan, Y., Sun, X., and Yuan, Q.:** Establishing an artificial pathway for efficient biosynthesis of hydroxytyrosol, ACS Synth. Biol., **7**, 647–654 (2018).

54. **Liu, X., Li, X. B., Jiang, J., Liu, Z. N., Qiao, B., Li, F. F., Cheng, J. S., Sun, X., Yuan, Y. J., Qiao, J., and Zhao, G. R.:** Convergent engineering of syntrophic *Escherichia coli* coculture for efficient production of glycosides, Metab. Eng., **47**, 243–253 (2018).

55. **Liu, H., Tian, Y., Zhou, Y., Kan, Y., Wu, T., Xiao, W., and Luo, Y.:** Multi-modular engineering of *Saccharomyces cerevisiae* for high-titre production of tyrosol and salidroside, Microb. Biotechnol., **14**, 2605–2616 (2021).

56. **Yang, H., Xue, Y., Yang, C., Shen, W., Fan, Y., and Chen, X.:** Modular engineering of tyrosol production in *Escherichia coli*, J. Agric. Food Chem., **67**, 3900–3908 (2019).

57. **Xue, Y., Chen, X., Yang, C., Chang, J., Shen, W., and Fan, Y.:** Engineering *Eschericha coli* for enhanced tyrosol production, J. Agric. Food Chem., **65**, 4708–4714 (2017).

58. **Xu, W., Yang, C., Xia, Y., Zhang, L., Liu, C., Yang, H., Shen, W., and Chen, X.:** High-level production of tyrosol with noninduced recombinant *Escherichia coli* by metabolic engineering, J. Agric. Food Chem., **68**, 4616–4623 (2020).

59. **Ruan, X., Zhang, S., Song, W., Liu, J., Chen, X., Liu, L., and Wu, J.:** Efficient synthesis of tyrosol from L-tyrosine via heterologous Ehrlich pathway in

Escherichia coli, Chin. J. Chem. Eng., **47**, 18–30 (2022).

60. **Gustavsson, M., Hörnström, D., Lundh, S., Belotserkovsky, J., and Larsson, G.:** Biocatalysis on the surface of *Escherichia coli*: melanin pigmentation of the cell exterior, Sci. Rep., **6**, 36117 (2016)
61. **Choi, K. Y.:** Bioprocess of microbial melanin production and isolation, Front. Bioeng. Biotechnol., **9**, 765110 (2021).
62. **Singh, S., Nimse, S. B., Mathew, D. E., Dhimmar, A., Sahastrabudhe, H., Gajjar, A., Ghadge, V. A., Kumar, P., and Shinde, P. B.:** Microbial melanin: recent advances in biosynthesis, extraction, characterization, and applications, Biotechnol. Adv., **53**, 107773 (2021).
63. **Zhang, H. and Wang, X.:** Modular co-culture engineering, a new approach for metabolic engineering, Metab. Eng., **37**, 114–121 (2016).
64. **Wang, R., Zhao, S., Wang, Z., and Koffas, M. A. G.:** Recent advances in modular co-culture engineering for synthesis of natural products, Curr. Opin. Biotechnol., **62**, 65–71 (2020).